Assessing extracellular vesicles as biological indicators for placental complications in the mouse

Elaine Lee

Division of Experimental Medicine

McGill University, Montreal, QC, Canada

November 2024

A thesis submitted to McGill University in partial fulfillment of the requirements of the degree of Master of Science

TABLE OF CONTENTS

ABSTRACT

Abnormal placental development and function are associated with various pregnancy complications, such as preeclampsia and intrauterine growth restriction. However, due to ethical concerns, directly obtaining placental samples during gestation for the early diagnosis and treatment of these pathologies remains largely unrecommended. Recently, nanoparticles known as extracellular vesicles (EVs) have demonstrated roles in mediating maternal-fetal crosstalk during placentation and have been actively explored as potential biomarkers for associated complications. Because previous studies have also reported the presence of various tissue-derived EVs in the circulation, the analysis of placental EVs in the plasma has been proposed as a minimally invasive strategy that could provide indirect insight into the maternal-fetal interface for diagnostic purposes. In this study, we aimed to explore the feasibility of this approach by first characterizing placental EVs obtained from a uterine *Nodal* knockout mouse model that recapitulated many abnormal placental phenotypes, such as impaired fetal growth, reduced decidual thickness, vascularization changes within the labyrinth, increased inflammation, and alterations to the composition of immune cell populations. Analysis of the EV cargo revealed the differential expression of numerous proteins and microRNAs involved in organ development, angiogenesis, metabolism, and immunomodulation between the knockout and control mice. Because the dysregulation of these processes mapped to phenotypic abnormalities actually observed in the *Nodal* knockout females, these findings validated the ability of the EVs to indicate the presence of placental defects through molecular changes in their cargo contents. Furthermore, the identification of specific cargo components that have previously been implicated in the pathophysiology of numerous placental complications highlighted the potential clinical applicability of these nanoparticles as disease biomarkers capable of monitoring maternal and fetal health during pregnancy to improve overall reproductive outcomes.

RÉSUMÉ

Les anomalies placentaires sont associées à diverses complications de grossesse telles que la pré-éclampsie et le retard de croissance fœtale. Cependant, le prélèvement d'échantillons placentaires pendant la grossesse pour le diagnostic précoce et le traitement de ces pathologies n'est pas recommandé pour des raisons éthiques. Récemment, il a été démontré que des nanoparticules appelées vésicules extracellulaires (VE) jouaient un rôle de médiateur dans les processus impliqués dans la placentation et leurs rôles en tant que biomarqueurs potentiels pour les complications associées a été exploré. Des études antérieures ont également démontré la présence de divers VE dérivés de tissus dans la circulation sanguine. Ainsi, l'analyse des VE placentaires dans le plasma a été proposée comme une stratégie peu invasive qui pourrait donner un aperçu de l'interface materno-fœtale à des fins de diagnostic. Nous avons cherché à explorer la faisabilité de cette approche en caractérisant les VE placentaires d'un modèle de souris knock-out *Nodal* utérin qui présente de nombreux phénotypes placentaires anormaux, tels qu'une croissance fœtale altérée, une épaisseur déciduale réduite, des changements de vascularisation dans le labyrinthe, une augmentation de l'inflammation et une altération des populations de cellules immunitaires. L'analyse des VE a révélé l'expression différentielle de nombreuses protéines et microARNs impliqués dans le développement des organes, l'angiogenèse, le métabolisme et l'immunomodulation chez les souris knock-out. Étant donné que la dysrégulation de ces processus correspond aux anomalies phénotypiques observées chez les femelles knock-out *Nodal*, ces résultats ont validé la capacité des VE à refléter la présence de défauts placentaires par le biais de changements dans leur contenu. De plus, l'identification de composants spécifiques des VE qui jouent un rôle dans la physiopathologie de nombreuses complications placentaires a mis en évidence l'applicabilité clinique potentielle de ces nanoparticules en tant que biomarqueurs permettant de surveiller la santé maternelle et fœtale pendant la grossesse afin d'améliorer les résultats globaux en matière de procréation.

ACKNOWLEDGEMENTS

I wish to first express my deepest gratitude for my supervisor, Dr. Daniel Dufort, who has guided me through this academic journey. Your consistent support and confidence in my abilities have served as a powerful source of strength that helped me persevere through obstacles and grow as an aspiring scientist. Thank you for this wonderful and invaluable experience.

I would like to extend my gratitude to my advisory committee members, Dr. Rima Slim, Dr. Makoto Nagano, and Dr. Bruce Mazer for their advice and expertise, which has ensured the quality of the presented work. Additionally, I would like to thank the members of the Dufort Lab whom I had the pleasure of meeting during my studies. To Rose-Andréa Corneli, Neha Kamath, Sarah Yull, Dr. Laura Girardet, Dr. Laurie Pinel, Dr. Shiva Shafiei, and Dr. Parinaz Kazemi, your support, encouragement, and friendship made my master's so fulfilling and it was a privilege working with such an amazing group of individuals. I would like to express my appreciation to Dr. Parinaz Kazemi in particular, who directly assisted me throughout my project. This work would not have been possible without your mentorship.

Many of the presented experiments were only achieved with the help from some incredibly skilled personnel and technological platforms based at McGill University, the Research Institute of the McGill University Health Centre (RI-MUHC), and Génome Québec. I would like to take this time to thank Dr. Janusz Rak, Dr. Nadim Tawil, and Laura Montermini from the RI-MUHC Centre for Applied Nanomedicine; Amy Wong and Lorne Taylor from the RI-MUHC Proteomics and Molecular Analysis Platform; the Facility for Electron Microscopy Research of McGill University; Daniel Jimenez from the RI-MUHC Bioinformatics Platform; and the Centre d'expertise et de services Génome Québec for their assistance in collecting and analyzing the data for this project.

Finally, I would like to express a heartfelt thank you to some of the closest people in my life. To my best friend, Nivi Rasiah, thank you for being my biggest cheerleader even when living thousands of miles away. Your love and support will always mean everything to me. And to my parents, Soyeon Ahn and Sanghun Lee, thank you for always motivating me to exceed my personal best and to never limit my dreams – this thesis is dedicated to the both of you.

CONTRIBUTION OF AUTHORS

The MSc. candidate Lee E., conducted the experiments, data analyses, and figure preparations for this manuscript with the assistance of postdoctoral fellow, Kazemi P. The exceptions are listed below. The NTA and TEM experiments presented in Figures 8A and 8C were performed by Kazemi P. with guidance from the Centre for Applied Nanomedicine and the Facility for Electron Microscopy Research of McGill University respectively. The LC-MS data presented in Figures 9-13 was obtained with assistance from the Proteomics and Molecular Analysis Platform at the Research Institute of the McGill University Health Centre. The miRNA library preparation and next-generation sequencing experiments presented in Figures 14-17 were performed with assistance from the Centre d'expertise et de services Génome Québec. The data analyses for Figures 14-17 and the figure preparations for Figures 15A and 17 were done with assistance from the Bioinformatic Platform at the Research Institute of the McGill University Health Centre. The manuscript was written and edited by Lee E. and Dufort D.

TABLE OF FIGURES

1. INTRODUCTION

1.1 Mammalian Pregnancy

Pregnancy is an essential reproductive process that ensures the propagation of progeny and genetic information for thousands of species (Evans & Ganjam, 2011). While there are nuanced interspecific differences in how pregnancy manifests and progresses physiologically, many of the general stages remain consistent for most mammals (Abbot & Rokas, 2017; Ochoa-Bernal & Fazleabas, 2020).

For a pregnancy to occur, the maternal and paternal gametes, also known as oocytes and spermatozoa respectively, must first fuse in the oviduct following copulation (Ochoa-Bernal & Fazleabas, 2020). This event is more formally known as fertilization and it enables the formation of the zygote, which then undergoes several series of cell divisions to form the blastocyst as it travels to the uterus. Upon reaching the uterus, the blastocyst integrates itself within the uterine wall with the aid of coordinated embryonic and maternal signals through a process known as implantation, which marks the successful establishment of a pregnancy (Kim & Kim, 2017). To support the implanted blastocyst, the maternal uterine tissue itself also undergoes numerous morphological and functional changes to form the decidua in a process called decidualization (Ochoa-Bernal & Fazleabas, 2020). This initiates the subsequent development of the placenta, establishing an interface through which the fetus can obtain nutrients and other resources necessary for its growth and development during gestation (Favaro et al., 2014; Gude et al., 2004). Pregnancy is finally concluded upon activation of the parturition cascade, which promotes the release of numerous cytokines and endocrinological signals to help expel the fetus from the maternal reproductive tract (Fig. 1) (Keelan et al., 2003).

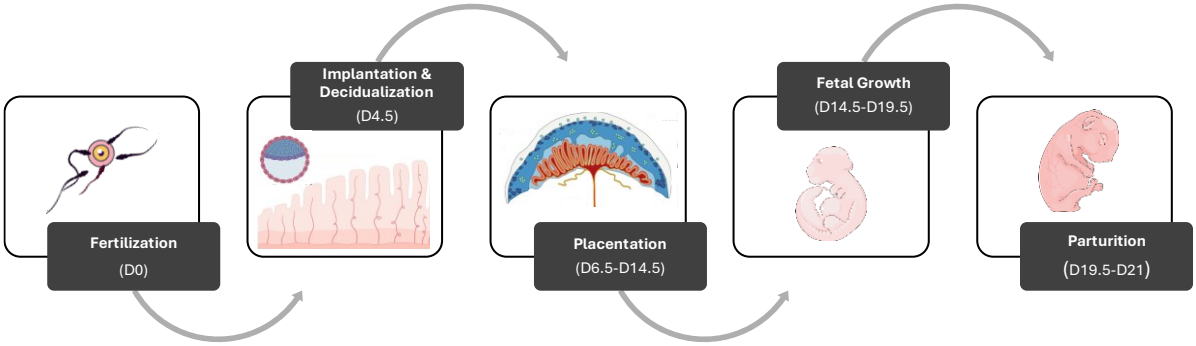

Figure 1. Pregnancy timeline in the mouse: Fertilization in the oviduct generates a diploid cell known as a zygote (D0), which undergoes numerous cell divisions to become a blastocyst as it

travels to the uterus to implant and establish a pregnancy within the mouse (D4.5). This initiates the process of decidualization, which transforms the maternal uterine environment to support the embryo during early gestation. The placenta then forms to provide an interface for communication and resource exchange between the mother and the fetus (D6.5-D14.5), which further advances fetal growth (D14.5-D19.5). Pregnancy is completed upon expulsion of the fetus during parturition (D19.5-D21). Figure created using images from (Hemberger et al., 2020; V. Jain et al., 2022; Shi et al., 2021) and those provided by Servier Medical Art (Servier; https://smart.servier.com/), licensed under a Creative Commons Attribution 4.0 Unported License.

As highlighted above, pregnancy is a complex biological phenomenon comprised of several key steps that must be fulfilled to ensure the proper development of the fetus as well as the health and safety of the mother. While complications can arise at any stage, many of those with severe pathological manifestations and poor maternal and neonatal outcomes have been affiliated with the period during which the placenta forms in particular (Norwitz, 2006). Because of this, extensive research efforts have been made to study the underlying mechanisms of placental development and its associated pathologies using a variety of experimental models, such as mice due to their genetic malleability and capacity to closely recapitulate human pregnancy (Aguilera et al., 2022; Bryda, 2013).

1.2 Placentation

1.2.1 Placental development in the mouse and its role in pregnancy

The placenta is a fetal-derived organ that is essential for the progression of pregnancy and fetal development. By anatomically intersecting the maternal uterus and fetal membranes, the placenta mediates various specialized functions, such as nutrient uptake and delivery, gas exchange, waste removal, and hormone production to adapt the maternal environment to support pregnancy maintenance (Burton & Fowden, 2015; Gude et al., 2004). Additionally, the placenta regulates the immune microenvironment to promote maternal immunotolerance, enhance the development of the fetal immune system, and protect the fetus from harmful pathogens (Ding et al., 2022; Smith et al., 2021, p. 17). Because of the importance of its functions, it is not surprising that one of the key stages of pregnancy is when placenta forms, which is a period formally known as placentation (Fig. 2).

Upon fertilization, the blastocyst that is formed consists of an outer layer of cells referred to as the trophectoderm, which encapsulates a cluster of cells known as the inner cell mass (Hemberger et al., 2020). Following implantation on embryonic day 4.5, the cells of the inner cell mass distinguish themselves into the epiblast and primitive endoderm. Concurrently, the polar trophectoderm adjacent to the inner cell mass proliferates to form the extraembryonic ectoderm and ectoplacental cone while the mural trophectoderm not in contact with the inner cell mass differentiates into trophoblast giant cells, which invade the decidua to connect between the maternal and fetal tissues (Hemberger et al., 2020; Watson & Cross, 2005). At embryonic day 6.5-7, the extraembryonic mesoderm forms from the epiblast and proliferates with the extraembryonic ectoderm to generate the anterior and posterior amniotic folds respectively, which subsequently combine to create the chorion (Simmons, 2014). During this time, the allantois also emerges from the extraembryonic mesoderm to link the developing placental vasculature to the yolk sac and fetal blood networks. As the allantois grows, it adheres to the chorion by embryonic day 8.5 in a process known as chorioallantoic attachment (Watson & Cross, 2005). The chorion then involutes to form the primary villi, which create a space where the allantoic cells making up the fetal blood vessels can migrate to bring them closer to the maternal blood sinuses (Simmons, 2014; Watson & Cross, 2005). This establishes the main architecture of the placental labyrinth, and as the chorion trophoblasts surrounding the fetal blood vessels fuse and differentiate into a cell type known as syncytiotrophoblasts, the labyrinth becomes a functionally active interface through which resource exchange can occur (Hemberger et al., 2020; Simmons, 2014). During the last stage of placentation from embryonic day 10-14.5, the placenta continues to grow and become more morphologically intricate through the development of the structurally supportive spongiotrophoblast cell layer from the ectoplacental cone and through increased branching of the labyrinthine blood vessels (Hemberger et al., 2020; Watson & Cross, 2005). Additionally, the generation of endocrinologically active and nutrient storing glycogen trophoblast cells from the spongiotrophoblast layer enables the placenta to become more functionally efficient, which ultimately aids in its ability to support fetal development and survival during pregnancy (Simmons, 2014).

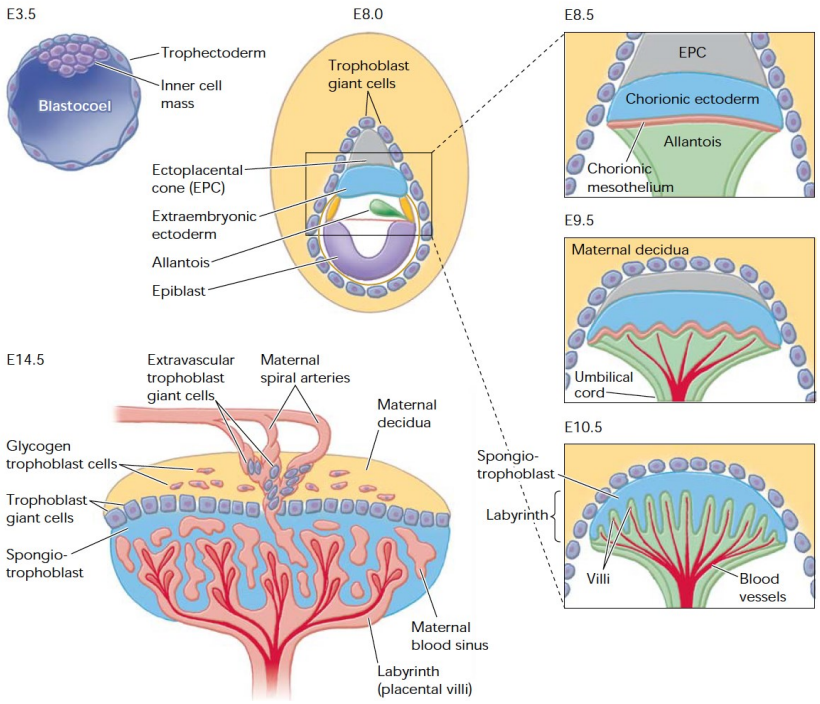

Figure 2. Placentation in the mouse: Upon implantation, the blastocyst undergoes extensive proliferation and differentiation to form the extraembryonic lineages that later produce the cellular components of the placenta. Notably, at embryonic day (E) 8.5, the chorion and the allantois adhere to one another to initiate the vascularization of the placenta through the development of the labyrinth layer. This is followed by accelerated tissue growth and enhanced differentiation of the various trophoblast cell types, which enables the placenta to become a mature and functionally active organ by E14.5. Figure from (Watson & Cross, 2005).

1.2.2 Placental complications

Because of its essential role in mediating maternal-fetal interactions during pregnancy, perturbations to placental development and function have been associated with numerous high-risk pregnancy complications in humans (Hemberger et al., 2020). One such complication that is observed in 10-15% of pregnancies is intrauterine growth restriction (IUGR), which is a pathological phenotype defined by fetal growth that is below the standard projected rate for the specified pregnancy timepoint (Armengaud et al., 2021; Mandruzzato et al., 2008). IUGR can occur due to various reasons, such as chromosomal and congenital abnormalities, infections, and maternal comorbidities like hypertension or diabetes (Sharma et al., 2016). However, in most cases, IUGR is caused by placental abnormalities that result in a maladaptive in-utero

environment that prevents the fetus from receiving all the resources necessary for its normal growth and development (Armengaud et al., 2021; Sharma et al., 2016). Another prevalent pregnancy complication that affects up to 2-10% of expectant mothers after 20 weeks of gestation is preeclampsia (Khan et al., 2022). Clinically, preeclampsia is typically characterized by the combined presence of newly onset hypertension, proteinuria, and other markers of systemic organ damage, such as low platelet counts and elevated liver enzyme activity (Khan et al., 2022; S. Rana et al., 2019). Similar to IUGR, preeclampsia has multiple underlying causes that include genetic variations of antiangiogenic factors, oxidative stress, inflammation, and maternal comorbidities like diabetes, obesity, renal disease, or chronic hypertension (S. Rana et al., 2019). Among the potential causes for preeclampsia, the most well-characterized is placental ischemia or reduced placental blood flow caused by the abnormal differentiation and activity of trophoblasts responsible for maternal vessel remodeling (Huppertz, 2008). This is believed to increase the release of antiangiogenic factors, such as sFLT and sENG, into the maternal circulation to promote the deleterious systemic effects commonly observed with this condition (Huppertz, 2008; S. Rana et al., 2019).

Because many pregnancy complications have etiological links to impaired placentation, direct analysis of the placental tissue during pregnancy has been proposed as a more effective and accurate approach for the early diagnosis of these pathologies. The only prenatal procedure currently practiced to obtain placental samples during pregnancy is chorionic villus sampling (CVS), which is a technique performed between 10-13 weeks of gestation to biopsy the placenta (Jones & Montero, 2022). It is typically performed for prenatal genetic testing only when a patient exhibits risk indications, such as an abnormal non-invasive prenatal genetic screen result, ultrasound abnormalities, history of a previous child with chromosomal abnormalities, or if the parent is a known carrier of a genetic disorder. The procedure can be performed transabdominally where a spinal needle containing tissue culture media is inserted into the placenta through the abdomen under the continued guidance of an ultrasound, or transcervically where a specialized catheter containing tissue culture media is inserted into the vagina to access the placenta (Jones & Montero, 2022). While generally considered to be safe when performed correctly, the CVS procedure has multiple reported risks due to its invasiveness, which include pregnancy loss, bleeding, infection, membrane rupture, leakage of amniotic fluid, and introduction of fetal limb defects (Jones & Montero, 2022; Salomon et al., 2019). Combined with

the strict indications that must be met for the procedure to be administered, many patients are unable to access the CVS test, which leads to many cases being left undiagnosed until it is too late (Jones & Montero, 2022). More minimally invasive diagnostic methods are available for specific conditions, such as ultrasound estimation of neonatal weight for IUGR, or blood pressure and urine tests for preeclampsia (S. Rana et al., 2019; Sharma et al., 2016). However, these options are unable to directly analyze the placenta and are still only offered when risk indications or symptoms are presented, at which point the condition has typically already advanced too far for preventative measures to be taken. Because of this, there is a significant unmet need for a minimally invasive diagnostic strategy that can analyze the placenta early in pregnancy regardless of a patient's risk profile in order to better monitor and detect cases of placental complications.

1.3 Extracellular Vesicles

1.3.1 EV subtypes and biogenesis

Extracellular vesicles (EVs) are cell-derived membranous particles that are unable to self-replicate and are nanosized in scale, generally ranging from 30-1000 nm in diameter (van Niel et al., 2018; Welsh et al., 2024). While originally thought to be only involved in cell waste trafficking and removal, the identification of various membrane and intraluminal cargo macromolecules, such as proteins, nucleic acids, and lipids, indicated larger functional roles for EVs in intercellular communication and the regulation numerous biological processes (Hessvik & Llorente, 2018).

EVs can be categorized into different groups based on their size and how they are generated (Fig. 3). Exosomes are generally small EVs that range from 30-200 nm in size (van Niel et al., 2018; Welsh et al., 2024). To generate exosomes, specialized organelles involved in intracellular trafficking known as endosomes first mature by undergoing membrane invagination to generate intraluminal vesicles (ILVs) that contain cargo macromolecules (van Niel et al., 2018). The formation of the mature endosome, or multivesicular body (MVB), is believed to occur through the combined interaction of several mechanisms. One mechanism utilizes the ESCRT machinery, which consists of four protein complexes (ESCRT-0, ESCRT-I, ESCRT-II,

ESCRT-III) and their associated accessory proteins. The ESCRT-0 and ESCRT-I complexes are thought to cluster EV cargo components onto MVB membrane microdomains and recruit the ESCRT-III complex through ESCRT-II to promote the internal budding of these microdomains to generate ILVs (Colombo et al., 2013). MVB biogenesis can also occur in an ESCRT-independent manner through the generation of ceramide lipids or tetraspanin protein clusters, which impose an inward negative curvature on the endosomal membrane to form the ILVs (Kaltenegger et al., 2021; Trajkovic et al., 2008; van Niel et al., 2011). Once formed, the MVB is either directed to the lysosome for degradation or the plasma membrane for exosome secretion by interacting with the actin cytoskeleton in a highly regulated manner that depends on the composition of proteins present on the MVB membrane (Hessvik & Llorente, 2018). For example, proteins with a ubiquitin-like modification known as ISGylation are believed to designate MVBs for degradation by promoting its fusion with lysosomes, while enrichment of the actin-binding protein cortactin or Rab GTPases, RAB27A/B, have been found to rearrange the cytoskeleton to promote MVB docking to the plasma membrane (Ostrowski et al., 2010; Sinha et al., 2016; Villarroya-Beltri et al., 2016). MVBs that are trafficked to the plasma membrane undergo fusion with the assistance of SNARE proteins, which form complexes to bring membrane sections into close contact with one another (Jahn et al., 2024; van Niel et al., 2018). Through the activation of small GTP-binding proteins like ARF6, membrane fission then occurs via actin-myosin contractions to release the ILVs into the extracellular milieu as exosomes (Muralidharan-Chari et al., 2009; van Niel et al., 2018).

Microvesicles are a larger subtype of EVs that are 200-1000 nm in size and are produced from plasma membrane budding (van Niel et al., 2018; Welsh et al., 2024). Its primary biogenesis mechanism is believed to depend on the activation of Ca^{2+}-dependent enzymes, such as scramblase and calpain, which rearrange the phospholipids of the membrane bilayer in a manner that reduces lipid asymmetry and subsequently promotes the outward bending of the plasma membrane to form the microvesicles (Fox et al., 1991; van Niel et al., 2018; Wu et al., 2020). Transforming the lipid composition of the plasma membrane by enriching it with cholesterol or ceramide has also shown to promote the generation of microvesicles by altering the biochemical interactions between membrane components (Gills et al., 2012; Khatibzadeh et al., 2013; van Niel et al., 2018). Furthermore, restructuring and regulating the actin cytoskeleton through proteins such as the RHO family of small GTPases and ROCK have demonstrated

effects on membrane budding dynamics and microvesicles release (B. Li et al., 2012; van Niel et al., 2018).

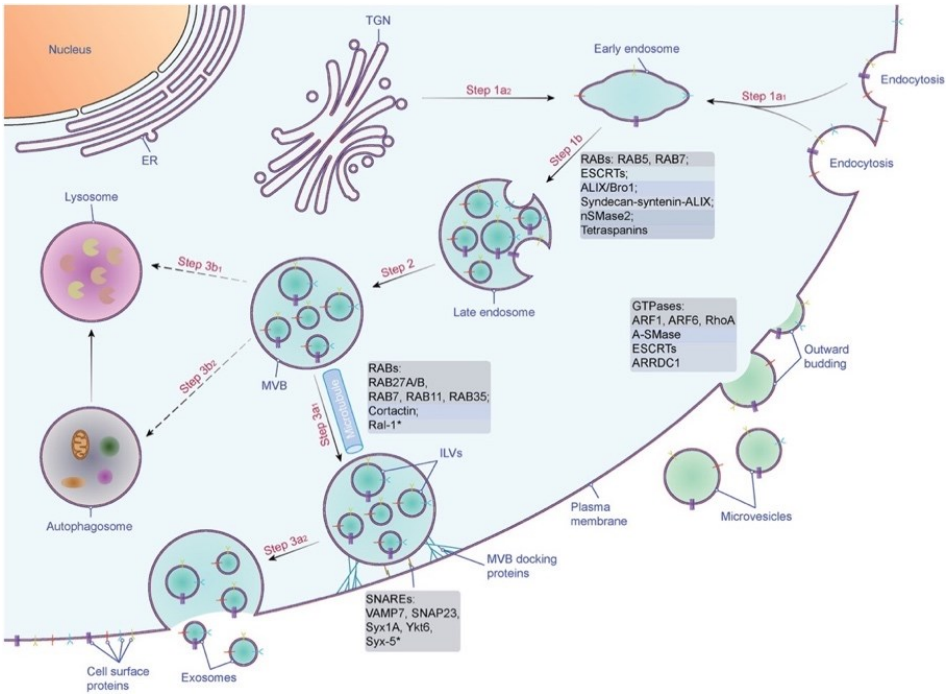

Figure 3. Biogenesis of extracellular vesicles: EVs can be generated through the endosomal pathway where mature endosomes or MVBs fuse with the plasma membrane to release the encapsulated ILVs into the extracellular space as exosomes. EVs can also be formed directly from the cytoplasm via budding of the plasma membrane as microvesicles. Both mechanisms depend on the complex coordination of numerous regulatory factors and interactions with various intracellular components. Figure from (Teng & Fussenegger, 2020).

1.3.2 EV cargo delivery and cellular uptake mechanisms

While EV subtypes differ in their biogenesis pathways, the mechanisms by which cargo molecules are targeted to these nanoparticles are similar and largely dependent on the type of cargo being sorted. RNAs are proposed to be sorted into EVs through the enriched presence of conserved sequences, like a 3'UTR motif, or by RNA-binding proteins present on the endosomal membrane (Oka et al., 2023; Villarroya-Beltri et al., 2013). Alternatively, cargo proteins are thought to be targeted to EVs by forming complexes with those already present on the endosomal and plasma membranes or by using post-translational modifications as membrane anchors (Katzmann et al., 2001; Kunadt et al., 2015; Larios et al., 2020). Finally, lipids are

believed to be sorted to EV biogenesis sites because of their high affinity for the lipid rafts on the endosomal and plasma membranes (Hessvik & Llorente, 2018; van Niel et al., 2018).

Regarding their functionality, studies found that EVs participated in intercellular signaling using two different strategies (Fig. 4). One way EVs have been found to activate downstream biological responses in recipient cells is through surface receptor interactions, such as those involving integrins, tetraspanins, lipids, lectins, proteogylcans, or extracellular matrix components (Altei et al., 2020; Christianson et al., 2013; Kwok et al., 2021; Morelli et al., 2004; van Niel et al., 2018). The second mechanism is by directly releasing their cargo contents into the cytoplasm of recipient cells, which can occur through direct fusion of the EV membrane with the plasma membrane of the recipient cell or through active internalization mechanisms, such as macropinocytosis, phagocytosis, or clathrin-mediated endocytosis (Fitzner et al., 2011; Parolini et al., 2009; Tian et al., 2014). In the case of the latter, internalized EVs must enter the endocytic pathway to integrate with MVBs where they are either degraded by lysosomes, re-secreted, or undergo back fusion to release their intraluminal contents into the cytoplasm of the recipient cells (Joshi et al., 2020; van Niel et al., 2018).

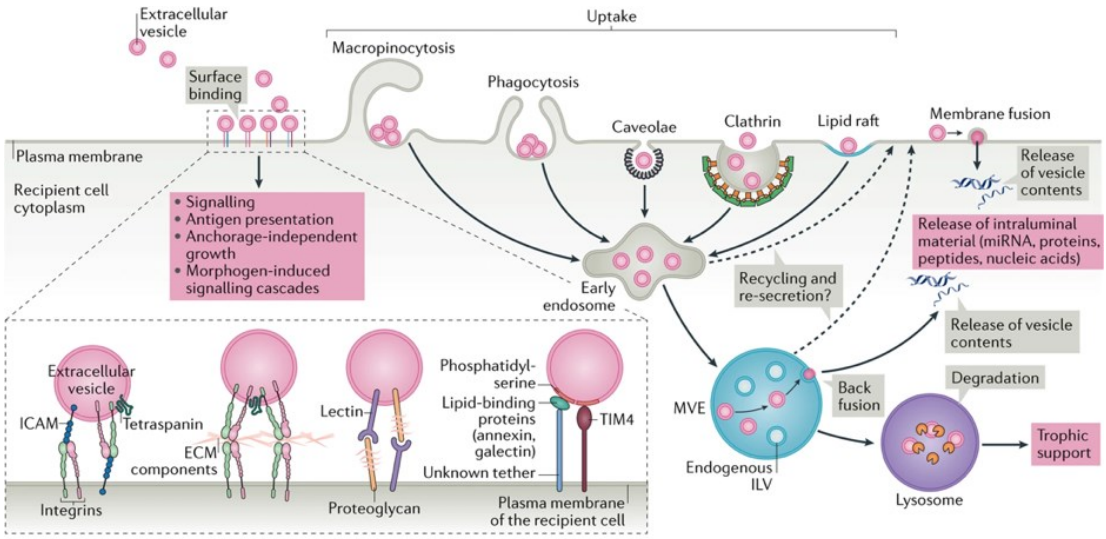

Figure 4. EV cellular uptake mechanisms: Released EVs can interact with recipient cells to elicit a biological response through several different mechanisms. Firstly, they can activate downstream signaling pathways by binding to surface receptors, such as integrins, lipids, and lectins. EVs can also use active internalization mechanisms, such as phagocytosis or clathrin-mediated endocytosis, where they will then become components of MVBs to either be degraded, re-secreted, or undergo back fusion to release their intraluminal contents into the cytoplasm of recipient cells. Finally, EVs can fuse with the plasma membrane of recipient cells to directly release their contents into the cytoplasm. Figure from (van Niel et al., 2018).

Regardless of the internalization mechanism, the release of the cargo contents into the cell allows the encapsulated macromolecules to exert a biological effect. This can include the regulation of gene expression by microRNAs (miRNAs), activation of signaling pathways by specific proteins, or the maintenance of metabolic homeostasis by lipid groups (Ghadami & Dellinger, 2023; Hánělová et al., 2024; O'Brien et al., 2020).

1.3.3 EVs and pregnancy complications

As aforementioned, EVs can impact biological processes by regulating their secretion as well as their encapsulated cargo. Among the biological processes implicated, several groups have demonstrated how EVs could mediate the pathophysiology of placenta-related pregnancy complications (Fig. 5). One way was by adversely affecting the placental vasculature. Under hypoxic conditions similar to those commonly observed in cases of preeclampsia or IUGR, EVs released by HTR-8/SVneo trophoblasts have been found to contain a miRNA known as miR-150-3p, which targeted the CHPF gene in endothelial cells to suppress their proliferative, migratory, and angiogenic properties (Sha et al., 2023). Plasma EVs from preeclamptic patients have also been found to inhibit the vasodilatory response of murine blood vessels by downregulating endothelial nitric oxide synthase levels, which is a phenotype associated with the placental ischemia characteristically seen in preeclampsia (Murugesan et al., 2022). Cumulatively, these findings highlighted how EVs could affect the development and functional capacity of the placental vasculature to precipitate the pathological outcomes commonly observed in associated complications.

EVs derived from patients with pregnancy complications, or those generated from cells exposed to maladaptive conditions, have also demonstrated negative effects on placental tissue morphogenesis. EVs from the term placenta of preeclamptic patients exhibited low levels of miR-101, which impaired trophoblast proliferation and migration when co-culture assays were performed (Cui et al., 2020). Interestingly, procoagulant EVs from mouse endothelial cells were also found to compromise the overall development and structural integrity of the placental interface in pregnant mice by excessively increasing the differentiation of the giant trophoblast and spongiotrophoblast cell types and impairing the differentiation of syncytiotrophoblasts (Markmeyer et al., 2021). Because alterations to the generation and expansion of different

placental cell types can impair the tissue's overall architecture and functionality, the elucidated findings demonstrated another way by which pathological EVs could compromise the normal progression of pregnancy through its effects on placentation.

Placental inflammation has also been linked to the development of adverse pregnancy outcomes and recent studies have suggested that EVs could precipitate this immunological phenotype. Procoagulant EVs from activated endothelial cells have been found to reduce embryo size, induce developmental malformations, diminish placental diameter, promote proteinuria, and increase the production of antiangiogenic factors in mice at mid-pregnancy. Further investigation of the underlying mechanism responsible for these signs of IUGR and preeclampsia revealed that the procoagulant EVs precipitated the observed phenotypes by activating the expression of inflammasome markers, such as NLRP3, Casp-1, and IL-1β, in trophoblast cells (Kohli et al., 2016). Changes to the cargo composition of trophoblast EVs from patients with recurrent miscarriage or preeclampsia have also been found to generate adverse changes to the immune cell landscape within the placenta. For example, increased levels of miR-196a-5p, tNA fragment 5'tRF-Glu-CTC, or sphingomyelin lipids were found to induce the M1 polarization of macrophages at the placental interface and excessively promote the production of numerous proinflammatory cytokines (Cooke et al., 2024; X. Liu et al., 2022; J. Zhang et al., 2022). Because inflammation is widely known to induce fetal distress and trophoblast dysfunction, the enhanced generation of proinflammatory cells within the placenta was proposed as a potential mechanism by which EVs could promote pathologies like recurrent pregnancy loss or preeclampsia. Overall, these observations demonstrated how EVs could foster negative placental phenotypes by disturbing the tissue microenvironment in addition to its development. This highlighted the multi-factorial role these nanoparticles could play in the pathophysiology of placenta-related complications, which further emphasizes their biological importance in the context of mammalian reproduction.

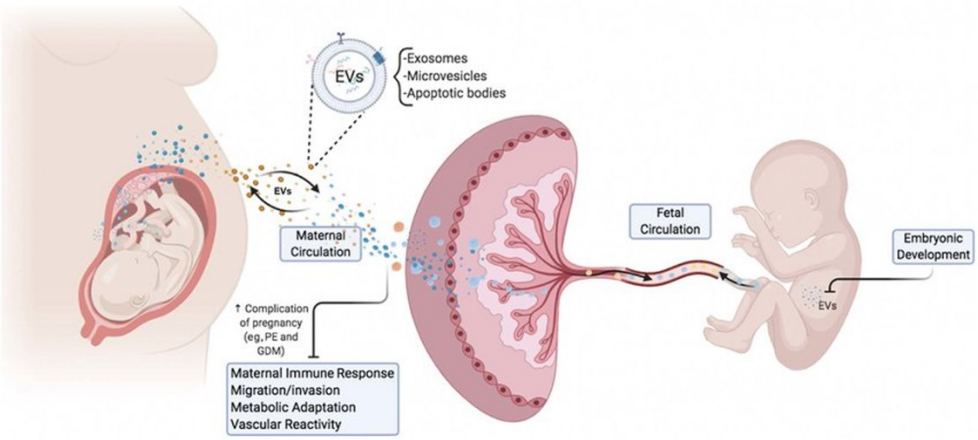

Figure 5. The role of EVs in pregnancy: EVs have been proposed as major mediators of pregnancy, especially during placentation. By transversing the placental interface, EVs can enter the fetal and maternal circulations to impact embryonic development and maternal processes respectively. Because of this, alterations to the concentration or contents of EVs have been found to contribute to the pathophysiology of various pregnancy complications, such as preeclampsia, IUGR, and gestational diabetes. Figure adapted from (Nakahara et al., 2020).

With the accumulation of evidence supporting EVs as major mediators of pregnancy complications, many have begun to explore their clinical applicability, especially as prospective disease biomarkers. Recently, EVs that retain the biological signature of their derived tissue of origin have been found in the circulation, which highlighted the potential for these nanoparticles to be used as a means to access pathologically implicated tissues in a minimally invasive manner for the diagnosis of various conditions (Zeng et al., 2022). In fact, several groups have attempted to isolate placental EVs from the plasma of patients with pregnancy complications using tissue-specific markers, such as placental alkaline phosphatase (PLAP) or syncytin-1, for this exact purpose because of the etiological role the placenta plays in many reproductive pathologies (Chaemsaithong et al., 2023; Levine et al., 2020). However, the inability to compare these EVs with those directly from the developing placentas of patients has challenged their validity as representative tissue factors capable of capturing the pathological environment responsible for the complication being investigated. While other studies have tried to provide more insight on EVs from the maternal-fetal interface, uncertainty regarding the utilized placental models and their ability to recapitulate specific disease conditions has questioned the accuracy of the currently available information. For example, EVs from placental cell lines are believed to be obtained under circumstances that fail to model the complexity of tissue and systemic biological

interactions while EVs from term human placenta are thought to be collected at a timepoint that differs from when the phenotypes manifest. To circumvent these limitations, murine models have been explored instead as an *in vivo* system that can realistically recapitulate human pregnancy while also providing easy access to the placental tissue at the time of disease onset. As these features can offer greater insights into the pathological placental environment responsible for the pregnancy complications being studied, many have begun to speculate whether EVs obtained from the developing placentas of murine models could be alternatively used to characterize prospective biomarkers, which can later be analyzed in patient plasma samples as a novel diagnostic approach.

1.4 Nodal

1.4.1 Nodal signaling pathway

While many mouse models of pregnancy pathologies have been introduced, one such model was generated by genetically dysregulating the Nodal signaling pathway.

Nodal is a 38-42 kDa homodimer protein that is a member of the TGF-β superfamily of signaling ligands (Le Good et al., 2005). Although Nodal is highly conserved across all vertebrates from zebrafish to humans, the functional role of this protein was first characterized through a transgenic screen of mice that were genetically manipulated using retroviral vectors (Shen, 2007). Mice with a recessive insertional mutation that mapped closely to the *Nodal* gene exhibited severe gastrulation abnormalities that led to embryonic lethality (Conlon et al., 1991; Zhou et al., 1993). Specifically, this mutation termed 413.d, impaired the organization of the primitive streak as well as the subsequent migration and formation of the meso-endoderm (Conlon et al., 1994). These initial findings confirmed the importance of this protein for embryogenesis, and following studies further delineated the role of Nodal in other developmental processes, such as left-right axis determination, neural patterning, and maintenance of stem cell pluripotency (Brennan et al., 2002; Londin et al., 2005; Vallier et al., 2005).

As a morphogen, Nodal is extracellularly secreted upon being synthesized into its precursor form, which is a disulfide-linked homodimer with post-translationally modified glycosylated sites (Le Good et al., 2005). To become functionally active, the N-terminal of the

Nodal proprotein must be enzymatically cleaved to release the 12 kDa C-terminal domain, which contains the mature ligand (Fig. 6) (Beck et al., 2002). This step is performed by convertases Furin and Pace4 with the assistance of a GPI-linked co-receptor known as Cripto, which recruits these enzymes and the Nodal precursor to the site where the mature ligand will bind to the recipient cell to initiate its signaling cascade (Beck et al., 2002; Yan et al., 2002). The site itself is a membrane-bound receptor complex comprised of a type I activin receptor like kinase (Alk4/7) and a type II activin receptor (ActRIIA/B) (Reissmann et al., 2001). Once Nodal is bound to the receptor complex, the ActRIIA/B subunit phosphorylates and activates Alk4/7 to initiate the subsequent phosphorylation of signal transducers Smad2/3 (Yeo & Whitman, 2001). The phosphorylated Smad proteins will then interact with Smad4 to promote their translocation to the nucleus where it will partner with additional transcription factors like FoxH1, Mixer, Milk, and p53 to facilitate DNA binding (Chen et al., 1997). This allows Nodal to regulate the expression of target genes, such as Sox17, FoxA, and Gata factors, as well as modulate the Fgf, Bmp, and Wnt signaling pathways to confer downstream biological effects (Meharwade et al., 2023; Soh et al., 2020; Wlizla & Zorn, 2015).

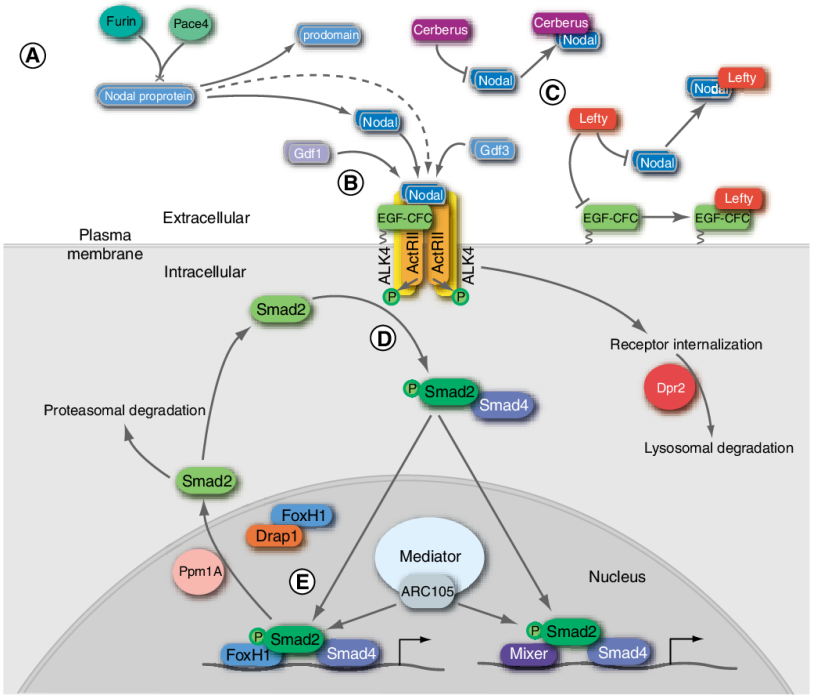

Figure 6. Nodal signaling pathway: Cleavage of the Nodal precursor protein by Furin and Pace4 releases the mature Nodal ligand, which binds to a membrane-bound receptor complex comprised of Alk4/7 and ActRIIA/B. This step is facilitated by a GPI-linked co-receptor known as Cripto, which recruits the enzymes and the Nodal precursor to the site where the mature Nodal ligand will bind to initiate the signaling cascade. Once Nodal is bound, the ActRIIA/B subunit

phosphorylates and activates Alk4/7, which subsequently phosphorylates signal transducers Smad2/3. Phosphorylated Smad2/3 will then interact with Smad4 to translocate to the nucleus where it will partner with additional transcription factors, such as FoxH1 and Mixer, to facilitate DNA binding and the expression of downstream target genes. Figure from (Shen, 2007).

The Nodal signaling pathway is highly controlled by various regulators (Schier, 2009). Nodal primarily self-regulates itself by activating the transcription of its own gene as well as its inhibitor Lefty, which binds and blocks the interaction between Nodal and its co-receptor Cripto. In addition to Nodal and Lefty, other regulators of the signaling pathway have been characterized over the years. Cerberus is a secreted inhibitor that directly sequesters the Nodal ligand while Dapper 2 antagonizes the Nodal pathway by promoting lysosomal degradation of the type I activin receptors. Downstream of the activin receptor complex, Nodal signaling can also be downregulated by nuclear phosphatase Ppm1A and ubiquitin ligase Ectodermin, which dephosphorylates Smad2/3 and ubiquitinates Smad4 respectively to block their interaction. Certain regulators can impair Nodal activity by altering the ability of its downstream effectors to associate with key transcription factors as well. For example, Zn-finger factor XFDL156 can bind the p53 transcription factor to block its association with Smad2 while Drap1 can sequester the FoxH1 transcription factor to impair its DNA-binding abilities. Alternatively, Nodal activity can also be upregulated at numerous points throughout the signaling cascade. Early in the pathway, Ras GTPase Rap2 can reactivate the Activin receptors to upregulate Nodal signaling while other TGF-β ligands, like Gdf1, can heterodimerize with Nodal to functionally enhance its activity. Nodal signaling transduction can also be increased by blocking the action of its inhibitors. For example, microRNAs, such as miR-430, have been shown to upregulate Nodal signaling by repressing Lefty transcripts while the FAM/Usp9x complex has been found to counter the ubiquitination of Ectodermin to promote the interactions between Smads 2, 3, and 4 downstream in the pathway as well (Tanaka et al., 2007).

1.4.2 The role of Nodal in pregnancy

The discovery of *Nodal* transcripts in the human endometrium during the proliferative and early secretory stages of the menstrual cycle suggested a larger role for the signaling

pathway in the field of female reproduction (Papageorgiou et al., 2009). In fact, the potential mechanisms by which Nodal can impact the proper progression of pregnancy from implantation to parturition have begun to be elucidated, and many of these findings were achieved using the uterine *Nodal* knockout (*Nodal* KO) mouse model developed by Dufort et al.

Notably, genetic abrogation of *Nodal* expression in the maternal uterus was found to yield many mid-pregnancy phenotypes representative of major reproductive pathologies. For example, starting from gestational day 10.5, embryos from the *Nodal* KO dams exhibited size and weight reductions indicative of an IUGR phenotype (Fig. 7A) (Park et al., 2012a; M. R. Rana, 2022). Additionally, analysis of the maternal and fetal tissues from these mice at the same timepoint revealed the differential expression of several genes that are commonly implicated in preeclampsia (unpublished data). When studying the implantation sites from the *Nodal* KO dams for potential morphological abnormalities that could account for the observed phenotypes, Dufort et al. found that the area of the maternal decidua appeared smaller throughout mid-pregnancy and the fetal portion of the placentas were also notably thinner by gestational day 14.5 (Park et al., 2012a; M. R. Rana, 2022). Placentas from these females also displayed major disorganization within the trophoblast giant cell and spongiotrophoblast layers as indicated by the abnormal staining patterns observed for the *Prl3b1*, *P-17*, and *TpbpA* markers respectively (Fig. 7B) (Park et al., 2012a). Furthermore, the *Nodal* KO females exhibited placental vasculature abnormalities by gestational day 14.5 as well, which was demonstrated by the significant reduction in maternal blood spaces and the over-expansion of fetal blood vessels seen in the labyrinth layers (Fig. 7C) (M. R. Rana, 2022).

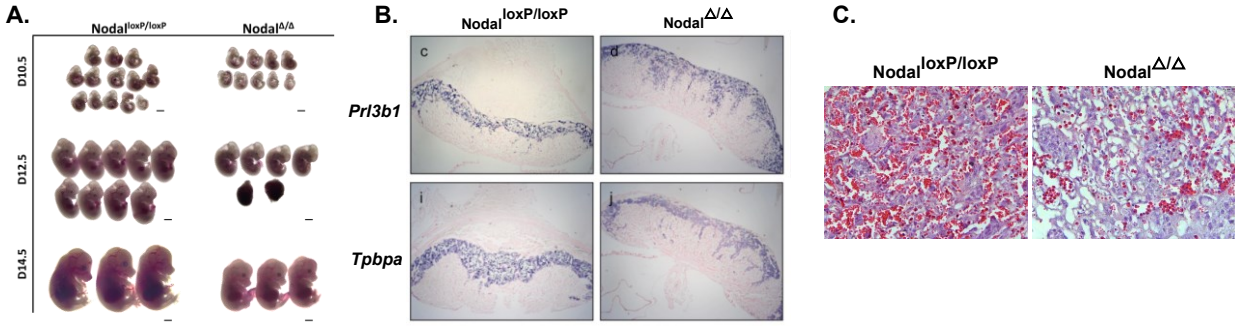

Figure 7. Mid-pregnancy phenotypes in *Nodal* KO dams: (A) Embryos from *Nodal* KO dams ($Nodal^{\Delta/\Delta}$) were smaller in size and weight than those from control females ($Nodal^{loxP/loxP}$) at the same mid-pregnancy timepoint. (B) Transverse sections of day 12.5 implantation sites from *Nodal* KO and control females were probed with different placental cell markers using in-situ hybridization. Extended staining of *Prl3b1* and *Tpbpa* into the fetal labyrinth indicated

disorganization and abnormal migration of trophoblast giant cells and spongiotrophoblasts respectively in the *Nodal* KO dams. (C) Histological images of the placental labyrinth were taken at day 14.5 and the maternal and fetal vascular regions were distinguished by maternal and fetal red blood cells (RBCs) respectively. Lower levels of unnucleated maternal RBCs and higher levels of nucleated fetal RBCs in the labyrinth of *Nodal* KO dams indicated abnormalities in the placental vasculature. Figure adapted from (Park et al., 2012a; M. R. Rana, 2022).

In addition to morphological differences, Dufort et al. also observed major physiological changes within the mid-pregnancy placentas of the *Nodal* KO dams. Through PCNA staining and the TUNEL assay, the cells within the maternal-fetal interface of the *Nodal* KO females were found to exhibit reduced proliferation and increased apoptosis levels respectively, which were believed to contribute to the diminished tissue areas previously described (Park et al., 2012a). The *Nodal* mutant females also displayed an elevation in proinflammatory cytokines, reduced neutrophil levels, and a decreased proportion of anti-inflammatory M2 macrophages at the maternal-fetal interface by gestational day 10.5, which indicated the presence of a dysfunctional placental immune environment (unpublished data). Interestingly, some of these phenotypes persisted and were compounded by an increased sensitivity to endotoxins, such as lipopolysaccharide, at later pregnancy timepoints as well, which further highlighted the extent to which compromised Nodal expression could impact the physiology of the placenta on an immunological level (Ayash et al., 2020).

The morphological and physiological changes observed in the *Nodal* KO mice demonstrated several means by which abnormal Nodal signaling could negatively impact placentation. By extension, because of the placenta's essential role in supporting fetal development and pregnancy maintenance, the elucidated findings also illustrated ways with which the Nodal signaling pathway could precipitate various pathological reproductive outcomes. With both the phenotypes and their underlying pathophysiological mechanisms characterized, the *Nodal* KO mice presented themselves as strong models for the next translational stage of research, which aimed to apply the obtained knowledge in a clinical context.

1.5 Rationale and Hypothesis

By mediating resource exchange and various physiological adaptations within the maternal microenvironment, the placenta distinguishes itself as an organ essential for fetal development and pregnancy maintenance. In fact, any biological changes that compromise placental formation or function have been recurrently linked to several high-risk pregnancy complications, such as IUGR and preeclampsia. Because of this, many have proposed that the analysis of the placental tissue during pregnancy could be a more effective and accurate diagnostic approach for many affected patients. However, due to the risks it presents to both the mother and the developing fetus, obtaining placental samples during gestation remains largely unrecommended, which has resulted in the delayed diagnosis of countless pathological cases. Consequently, there is a significant need for the development of an early and minimally invasive diagnostic strategy that can be readily accessed to maximize prevention and treatment opportunities for expectant mothers afflicted by these pregnancy complications.

Recently, cell-derived nanoparticles known as EVs have been explored as carriers for potential diagnostic biomarkers. Previous studies have demonstrated the active role EVs can play in mediating various processes involved in placentation both under normal and pathological conditions, such as tissue morphogenesis, vascularization, and immunoregulation. Supported by the finding that tissue-specific EVs can enter the systemic circulation to participate in long-range cell signaling, the analysis of placental EVs has been proposed as an ideal diagnostic strategy for many pregnancy complications due to their ability to provide close insight into the maternal-fetal interface while circumventing the risks associated with current techniques.

Concerns regarding the lack of information on the molecular profile of EVs directly from the developing placentas of patients at the time of disease onset has challenged the feasibility of the delineated approach. As a result, some have alternatively proposed the study of placental EVs in genetically engineered mice due to their ability to realistically model *in vivo* biological conditions while also providing easy access to the placental tissue for research purposes. One mouse strain that has been used to study mammalian reproduction was developed by knocking down the *Nodal* gene in the uterus. Maternal abrogation of Nodal signaling in these mice was found to precipitate numerous mid-pregnancy phenotypes indicative of dysfunctional placentation, such as trophoblast disorganization, abnormal vascularization, proinflammation, and impaired fetal growth. With an established model that presents signs of various reproductive

pathologies, we believed that the feasibility of analyzing EVs for the early diagnosis of associated complications could be preliminarily tested by first assessing if placental EVs could accurately capture the phenotypes observed in the *Nodal* KO mice at the time of sample collection around mid-pregnancy. We hypothesized that placental abnormalities caused by dysfunctional maternal Nodal signaling at mid-pregnancy can alter the EVs from the maternal-fetal interface in a manner that is detectable and predictive of the observed pathological phenotypes. To validate this research hypothesis, we aimed to:

(1) Characterize and compare the protein cargo of EVs derived from the maternal-fetal interface of control and *Nodal* KO mice at mid-pregnancy
(2) Characterize and compare the miRNA cargo of EVs derived from the maternal-fetal interface of control and *Nodal* KO mice at mid-pregnancy

Through the work presented in this thesis, we ultimately hope to delineate potential biomarker candidates that are indicative of placental dysfunction from the cargo of placental EVs derived from the *Nodal* KO dams. By doing this, we believe that we can help further advance the development of a novel diagnostic approach that is minimally invasive, and thus more readily accessible, to improve reproductive outcomes for patients with high-risk pregnancy complications worldwide.

2. METHODS AND MATERIALS

2.1 Generation of Nodal Mutant Mice

All experimental and animal handling protocols were approved by the Animal Care Committee at the Research Institute of the McGill University Health Centre and adhered to the regulations stipulated by the Canadian Council on Animal Care. To produce a mouse model that exhibits pregnancy abnormalities, adult female dams with a uterine-specific knockout of the *Nodal* gene were generated using the loxP-Cre recombinase system as previously described (Park et al., 2012b). In order to obtain the genotypes necessary to implement this site-specific gene editing approach, we utilized two mouse strains generously donated by two groups. E. J. Robertson's group generated and provided mice that possessed loxP sites flanking exons 2 and 3 of the *Nodal* gene ($Nodal^{loxP/loxP}$) on a mixed background (University of Oxford)(Lu & Robertson, 2004). Progesterone receptor (PR)-Cre mice ($Pgr^{Cre/+}$) on a C57BL6/129 background were generated and donated by F. J. DeMayo and J. P. Lydon (Baylor College of Medicine)(Soyal et al., 2005). The PR-Cre mouse line was selected for this study due to the strain's ability to target and restrict Cre-recombinase activity to maternal reproductive tissues where progesterone receptor expression is highly enriched (Soyal et al., 2005). Furthermore, as the PR-Cre mice themselves exhibited normal fertility, we could ensure that the reproductive phenotypes observed in this study were predominately due to the excision of the *Nodal* gene in maternal tissues (Mukherjee et al., 2006). $Nodal^{loxP/loxP}$ mice were crossed with $Pgr^{Cre/+}$ mice and appropriate breeding pairs were formed from subsequent offspring generations to generate the control females ($Nodal^{loxP/loxP}$, $Pgr^{+/+}$ henceforth referred to as CTL) and the homozygous *Nodal* mutant females ($Nodal^{loxP/loxP}$, $Pgr^{Cre/+}$ henceforth referred to as KO) used in this study.

2.2 Genotyping

To extract the DNA for genotyping, tail snips were obtained from the mice and digested in 300 µL of lysis buffer (100mM tris-HCl pH 8.0, 10mM EDTA pH 8.0, 0.5% Tween® 20, 0.5% Nonidet P-40) and 30 µL of 10 mg/mL of proteinase K (Roche, Basel, CH) at 55-60°C on a heat block overnight. Following overnight digestion, the samples were centrifuged at 13,000 rpm for 6 minutes. The $Nodal^{loxP}$ (290 bp) and $Nodal^{+}$ (220 bp) alleles were amplified by touchdown PCR on the T100 Thermal Cycler (1861096, Bio-Rad Laboratories, Inc., Hercules, CA, USA)

for 7 cycles at one setting (94°C for one minute, 58°C for 30 seconds, and 72°C for 30 seconds), then for 30 cycles at another setting (94°C for 30 seconds, 58°C for 30 seconds, and 72°C for 30 seconds) using the following primers: 5'-ATTCCAGCAGTTGAGGCAGA-3'and 5'-GCTATGCCACGCAGAACC-3'. The PR^{Cre} (570 bp) and PR^{+} (300 bp) alleles were amplified by standard PCR for 30 cycles (94°C for one minute, 60°C for 1 minute, and 72°C for 2 minutes) on the T100 Thermal Cycler with the following primers: 5'-ATGTTTAGCTGGCCCAATG-3'; 5'-TATACCGATCTCCCTGGACG-3'and 5'-CCCAAAGAGACACCAGGAAG-3'. Amplified bands were then run and visualized on a 1-2% agarose gel using gel electrophoresis to confirm of the genotype of the samples.

2.3 Mating and Manipulation of Transgenic Mice

Nodal CTL and KO females aged 8-24 weeks were mated overnight with wild-type CD1 males (Charles River Laboratories, Wilmington, MA, USA). The presence of a vaginal mucous plug the following morning was used as an indication that successful copulation had occurred, and these females were designated as being 0.5 days pregnant (D0.5). At day 10.5 of pregnancy (D10.5), the females were euthanized and uterine horns were collected then transferred to a petri dish containing 1× RPMI 1640 media (350-000 CL, WISENT Inc., Saint-Jean-Baptiste, CA) on ice.

2.4 Dissection and Preparation of Placental Tissue

From the collected uterine horns, the decidua and placenta from each implantation site were isolated and cleaved into quarter segments. To prepare the tissue for cell lysis, 55-100 mg of tissue was submerged and set aside in 1 mL of 1× RIPA buffer (9806, Cell Signaling Technology, Inc., Danvers, MA, USA) that contained 1× cOmplete™, Mini, EDTA-free Protease Inhibitor Cocktail (04693159001, Roche, Basel, CH) and 2mM of PMSF (P7626-1G, Sigma-Aldrich, St. Louis, MO, USA). Alternatively, to prepare the tissue for EV isolation, the cleaved segments were placed in 1× RPMI 1640 media with 20 µg/mL of Liberase™ TM (5401119001, Roche, Basel, CH) and 30 µg/mL of DNase I (DN25, Sigma-Aldrich, St. Louis, MO, USA) such that every 0.2 g of tissue was exposed to 2 mL of digestion media (Crescitelli et al., 2021). The tissue segments were digested for 30 minutes at 37℃, after which the media was pooled through

a 0.70 µm cell strainer and centrifuged for 15 minutes at 4℃ at 500×*g* to bring down any tissue fragments and cell debris (Crescitelli et al., 2021). This was followed by another round of centrifugation for 15 minutes at 4℃ at 2000×*g* to bring down any remnant debris present in the media (Crescitelli et al., 2021).

2.5 Isolation of Extracellular Vesicles

Following centrifugation to bring down media debris, the supernatant was filtered through a 0.45 µm filter and transferred to an Amicon Ultra-15 Centrifugal Filter, 100 kDa MWCO concentrating tube (UFC910024, MilliporeSigma, Burlington, MA, USA). Once the supernatant was concentrated to 500 µL, it was filtered through a qEVoriginal isolation column that recovers particles with sizes between 70-1000 nm (ICO-70, Izon Sciences Limited, Christchurch, NZ). The samples were filtered through the Izon column using 0.1-µm-filtered PBS and five fractions of 400 µL were collected and pooled for each sample. 10 µL from every pooled 2 mL sample was set aside for nanoparticle tracking analysis, and the remaining volume of each sample was then concentrated to 50-70 µL using an Amicon Ultra-0.5 Centrifugal Filter, 100 kDa MWCO concentrating tube (UFC510024, MilliporeSigma, Burlington, MA, USA). The final samples were stored at -80℃ until further analysis was performed.

2.6 Nanoparticle Tracking Analysis

To determine the size distribution and concentration of the particles present in the isolated samples, nanoparticle tracking analysis was performed using the NanoSight NS300 instrument (Malvern Panalytical, Malvern, UK). The samples were injected into the instrument with a 1 mL syringe at a speed of 25 µL/s after being diluted 400- to 2000-fold using 0.1-µm-filtered PBS to achieve an optimal field of view of 20 to 80 particles per frame. Five 30-second videos were acquired at a detection threshold of 5, a camera level of 14, a laser wavelength of 532 nm, and a temperature of 37℃. The NanoSight Software NTA 3.4 (version 3.4.4) was used for analysis of the instrument's measurements.

2.7 Transmission Electron Microscopy

To visualize the collected EVs, 5 µL of the sample was placed on top of a charged 200-mesh carbon-coated Cu grid for 5 minutes. The grid was washed three times with distilled water and then negatively stained with 2% uranyl acetate for 45 seconds to 1 minute. Excess solution present on the grid was blotted off using Whatman filter paper, and the grid was air-dried for 1 hour prior to imaging. The imaging was performed using the FEI Tecnai 12 BioTwin 120 kV TEM (Thermo Fisher Scientific Inc., Waltham, MA, USA) with the AMT XR80C CCD Camera System (AMT Imaging, Woburn, MA, USA) at the Facility for Electron Microscopy Research of McGill University.

2.8 Protein Extraction and Concentration Quantification

To extract protein from the placental cell lysis samples, the tissue that was previously submerged in 1× RIPA buffer was homogenized and placed on a plate rocker for 15 minutes at 4℃. The samples were then transferred to Eppendorf tubes and centrifuged for 10 minutes at 10,000×*g* at 4℃. The middle supernatant layer that contained protein was then collected and stored at -80℃ until further analysis was performed. To extract protein from EVs, the isolated EV samples were treated with the 1× RIPA buffer in a 1:1 ratio. Following protein extraction, 6 µL of each of the samples were diluted 60x with filtered PBS and the protein concentration was checked following the instructions outlined in the Micro BCA™ Protein Assay Kit (23235, Thermo Fisher Scientific Inc., Waltham, MA, USA). The absorbance of the samples was measured at a wavelength of 562 nm using the Infinite M200 PRO® NanoQuant microplate reader (Tecan Group Ltd., Männedorf, CH) and its corresponding i-control™ software (version 1.12.4.0).

2.9 Western Blotting

The concentrations of the samples were normalized by adjusting the volume of the sample and filtered PBS diluent accordingly. The samples were then treated with 2× Laemmli buffer containing β-mercaptoethanol in a 1:1 volume ratio and placed on a heat block at 95℃ for 5 minutes to allow for protein denaturation. The proteins were resolved on a 12% SDS-PAGE gel at 140 V and transferred to an Immun-Blot® PVDF membrane with a 0.2 µm pore size (1620177,

Bio-Rad Laboratories, Inc., Hercules, CA, USA) at 20 V overnight at 4℃. The membranes were blocked with 5% non-fat skim milk in 1× TBS-T for 2 hours and subsequently incubated with the primary antibodies of interest overnight at 4℃. To detect the expression of common EV markers, the following primary antibodies were diluted at the specified concentrations in 1× TBS-T: 1:500 dilution of rat anti-CD63 (143901, BioLegend, San Diego, CA, USA), 1:500 dilution of rat anti-TSG101 (934301, BioLegend, San Diego, CA, USA), 1:500 dilution of rat anti-CD9 (124802, BioLegend, San Diego, CA, USA), and 1:500 dilution of mouse anti-HSC70 (sc-7298, Santa Cruz Biotechnology, Inc., Dallas, TX, USA). Following incubation with the primary antibody, the membranes were rinsed 3 times in 5-minute intervals with 1× TBS-T and then incubated with the appropriate secondary antibody. The following secondary antibodies were diluted in blocking buffer at the specified concentrations: 1:5000 dilution of HRP-conjugated goat anti-rat IgG (112-035-003, Jackson ImmunoResearch Laboratories Inc., West Grove, PA, USA) and 1:2500 dilution of HRP-conjugated goat anti-mouse IgG (115-035-062, Jackson ImmunoResearch Laboratories Inc., West Grove, PA, USA). The membranes were rinsed again 3 times in 5-minute intervals with 1× TBS-T and treated with the Clarity™ Western ECL Substrate (1705061, Bio-Rad Laboratories, Inc., Hercules, CA, USA) for 5 minutes before being imaged using the Amersham™ Imager 600 (GE HealthCare Technologies, Inc., Chicago, IL, USA).

2.10 Liquid Chromatography-Mass Spectrometry (LC-MS) Proteomics

LC-MS proteomics analysis was performed by the Proteomics and Molecular Analysis Platform at the Research Institute of the McGill University Health Centre (RI-MUHC). The protein concentrations of the EV samples (N=4 of Controls; N=4 of *Nodal* KO) were normalized so that approximately 67 μg of protein were sent for each sample. The proteins for each sample were loaded onto a single stacking gel band to remove any lipids, detergents and salts. The gel band was reduced with DTT, alkylated with iodoacetic acid, and digested with trypsin. Extracted peptides were re-solubilized in 0.1% aqueous formic acid and loaded onto an Acclaim™ PepMap™ precolumn (75 μM ID × 2 cm C18 3 μM beads, Thermo Fisher Scientific Inc., Waltham, MA, USA) and then onto an Acclaim™ PepMap™ EASY-Spray™ analytical column (75 μM × 15 cm with 2 μM C18 beads, Thermo Fisher Scientific Inc., Waltham, MA, USA). The

peptides were then separated using a Dionex UltiMate 3000 UHPLC (Thermo Fisher Scientific Inc., Waltham, MA, USA) at 250 nL/min with a gradient of 2-35% organic (0.1% formic acid in acetonitrile) over 3 hours. Peptides were analyzed using a Thermo Scientific™ Orbitrap Fusion™ mass spectrometer (Thermo Fisher Scientific Inc., Waltham, MA, USA) operating at 120,000 resolution (FWHM in MS1) with HCD sequencing (15,000 resolution) at top speed for all peptides with a charge of 2+ or greater. The raw data was converted into a *.mgf format (Mascot generic format) so it can be searched in the Mascot 2.6.2 search engine (Matrix Science) to delineate mouse protein sequences (UniProt, 2023).

2.11 RNA Extraction

To extract total RNA, 45-50 µL of each EV sample (N=3 of Controls; N=3 of *Nodal* KO) was first treated with 20 µg/µL of proteinase K for 30 minutes at 37℃ to purify them of non-EV protein contamination (Ibrahim et al., 2024). The samples were then treated with 20 µg/µL of RNAse A (FEREN0531, Fisher Scientific International, Inc., Hampton, NH, USA) for 2 minutes at room temperature to eliminate any non-EV RNA contamination (Ibrahim et al., 2024). The QIAZol Lysis Reagent from the Qiagen miRNeasy Micro Kit (217084, QIAGEN N.V., Hilden, DE) was added to the samples in a 5:1 ratio and vortexed for 5 seconds before being kept at room temperature for 5 minutes. Chloroform was then added to the samples in a 1:5 volume ratio, vortexed for 15 seconds, and left to incubate for 3 minutes at room temperature. The samples were centrifuged for 15 minutes at 12,000×*g* at 4℃, and the resulting aqueous phase was removed and mixed with 1.5× 100% ethanol. The samples were transferred to the MinElute™ columns from the Qiagen miRNeasy Micro Kit and the instructions outlined in the kit were then followed to complete the RNA extraction.

2.12 RNA Concentration Quantification, Library Generation, and miRNA Sequencing

Quantification of the total RNA concentration, generation of the small RNA libraries, and the miRNA sequencing were performed by the Centre d'expertise et de services Génome Québec. The total RNA concentration was quantified using a NanoDrop Spectrophotometer ND-1000 (NanoDrop Technologies, Inc., Wilmington, DE, USA). Libraries were generated from 1000 ng of total RNA using the NEBNext Multiplex Small RNA Library Prep Kit for Illumina

(New England Biolabs, Ipswich, MA, USA), as per the manufacturer's recommendations. cDNA construct purification was performed using SparQ beads (QIAGEN N.V., Hilden, DE). Libraries were quantified using the KAPA Library Quantification Kits - Complete kit (Universal) (Kapa Biosystems, Wilmington, MA, USA) and the average size fragment was determined using a Fragment Analyzer instrument (Agilent Technologies, Inc., Santa Clara, CA, USA). The libraries were normalized and pooled. The pool was diluted to 650 pM using RSB Tween20 and a phiX library was used as a control and mixed with the libraries at a 5% level. The pool was loaded on a P1 NextSeq 2000 lane as per the manufacturer's instructions (Illumina, Inc., San Diego, CA, USA) and the run was performed for 2×100 cycles (paired-end mode). Program BCL Convert 4.2.4 was then used to demultiplex samples and generate FASTQ reads. The raw FASTQ files were initially processed with fastp to remove adapter sequences and ensure quality control. The resulting trimmed reads were subsequently input into the exceRpt pipeline for small RNA sequence identification and transcript quantification.

2.13 Bioinformatics and Statistical Analysis

For the proteomics data, the Mascot 2.6.2 search results were loaded onto the Scaffold Q+/Scaffold 5 software (version 5.2.2, Proteome Sciences) for quantitative analysis. The proteins were filtered to eliminate any proteins that had peptide reads missing in more than 50% of the replicates for either experimental group. The resulting protein list was checked against the National Center for Biotechnology Information (NCBI) Gene database (National Center for Biotechnology Information, 2004) and the TissueEnrich webtool (A. Jain & Tuteja, 2021) to confirm the tissue signature of the EVs. Differential expression analysis for the proteomics data was performed on Scaffold by calculating the fold change difference for all proteins between the *Nodal* CTL and KO EV samples as well as by implementing the Student's t-test. Proteins were differentially expressed between the *Nodal* CTLs and KOs if they displayed a fold change > 1.5 and a p-value < 0.05. Over-representation analysis for enriched gene ontology, phenotype, and disease terms was performed using the PANTHER (version 18.0) and MOET (version 2.0) online databases respectively (Mi et al., 2019; Thomas et al., 2022; Vedi et al., 2022).

For the miRNA-Seq results, small RNAs not classifed as miRNAs and miRNAs with transcript reads missing in more than 1/3 of the replicates for either experimental group were filtered out. Differential expression analysis on the resulting miRNA list was performed with the

DESeq2 R package using the raw count data generated by the exceRpt pipeline. The $\log_2$ fold change difference was calculated for all miRNAs and statistical significance was determined using the Wald test with Benjamini-Hochberg correction. miRNAs were differentially expressed between the two groups if they displayed a $\log_2$(fold change) > 1.5 and an adjusted p-value < 0.05. miRNA-gene interactions were annotated using multiMiR R package, which incorporated the miRTarBase database for validated target information. Associated target genes were subjected to over-representation analysis to elucidate enriched gene ontology, phenotype, and disease terms using the clusterProfiler R package and the MOET online database.

To generate the final list of biomarker candidates, a systematic literature review was performed for the proteins and target genes of miRNAs differentially expressed between the two groups to determine if they had any previously reported roles in placentation or related processes. Top biomarker candidates were also checked against publicly available RNA-Seq or microarray databases of placental samples from patients with pregnancy complications to determine if they were previously found to be dysregulated under real pathological conditions.

Figures were generated using the ggplot2, heatmap.2, pheatmap, igraph, and ggraph packages on R version 4.3.1.

3. RESULTS

3.1 Validate the successful isolation of tissue-derived placental EVs from mice at mid-pregnancy

3.1.1 Particles within the collected samples exhibit quantitative and qualitative features characteristic of EVs

To confirm the collected samples consisted of EVs, several orthogonal and complementary methods, such as NTA, TEM, and immunoblotting, were performed to define different EV identification parameters as recommended by the Minimal Information for Studies of Extracellular Vesicles (MISEV) 2023 guidelines (Welsh et al., 2024).

Using NTA, we found that the particles in the control samples had a mean diameter range of 161.4-182.9 nm and a mode diameter range of 106.5-125.4 nm (Fig. 8A). The particles in the *Nodal* KO samples had similar measurements as they displayed a mean diameter range of 156.7-188.8 nm and a mode diameter range of 105.4-115.9 nm. Because EVs are estimated to be 30-1000 nm in size, the NTA data validated that the isolated samples possessed EV-sized particles (van Niel et al., 2018; Welsh et al., 2024). Furthermore, the concentration range of the particles in the control and *Nodal* KO samples were approximated to be 2×10^{11}- 6×10^{11} particles/mL and 3×10^{11}- 9×10^{11} particles/mL respectively, which confirmed the comparable efficacy by which the protocol isolated EVs from both control and *Nodal* KO placentas. TEM analysis allowed us to visualize membranous spherical structures in the samples (Fig. 8C), which resembled previously published images of EVs (Rikkert et al., 2019). Along with the confirmed expression of common EV markers Cd63, Cd9, Tsg101, and Hsc70 in the samples via immunoblotting (Fig. 8B), these findings validated the successful isolation of EVs with the established protocols (Kowal et al., 2016).

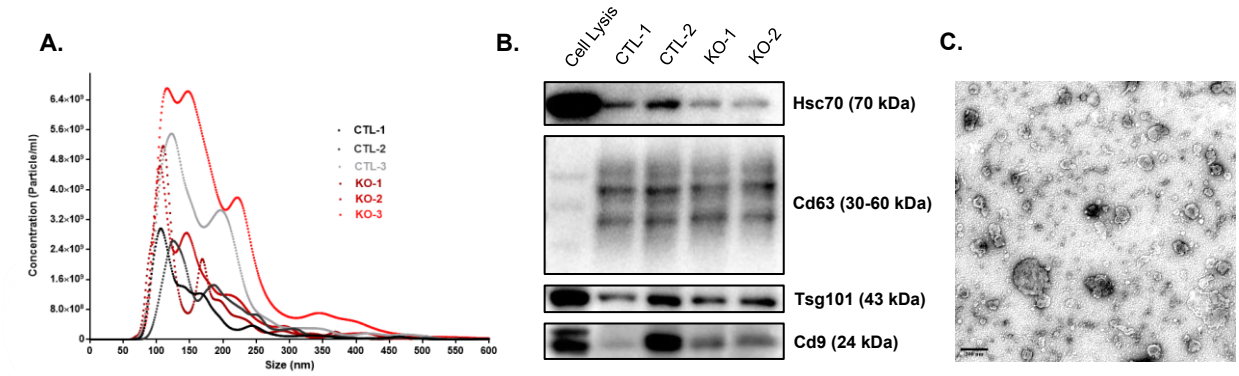

Figure 8. Collected particles exhibit size, protein markers, and morphological features characteristic of EVs: (A) Graphical representation of the NanoSight NS300 NTA data illustrating the concentration and size distribution of the particles present in the *Nodal* CTL (N=3) and KO (N=3) EV samples isolated from enzymatically digested D10.5 placentas. (B) Western blots displaying the expression of EV markers Hsc70, Cd63, Tsg101, and Cd9 in *Nodal* CTL (N=2) and KO (N=2) EV samples isolated from D10.5 placentas. Protein from homogenized D10.5 placental tissue ("Cell Lysis") was used as a positive control. The concentrations of the loaded protein samples were normalized so that approximately 25 μg of total protein was loaded for all samples. (C) TEM image of *Nodal* CTL EVs from enzymatically digested D10.5 placentas visualized using the FEI Tecnai 12 BioTwin 120 kV microscope. Scale bar represents 200 nm in the image.

3.1.2 The isolated EVs possess a strong placenta-specific tissue signature at the protein level

Since this study aimed to characterize EVs specifically derived from the maternal-fetal interface, we had to first confirm that the collected nanoparticles reflected their source tissue of origin by expressing markers distinctive to the placenta. At the miRNA level, only those from the chromosome 19 miRNA cluster (C19MC) have been previously characterized as placenta specific (Bentwich et al., 2005). However, because C19MC miRNAs are exclusively found in primates, we focused on protein placental markers instead to confirm the tissue origins of our murine-derived EVs. Proteins extracted from the EVs were analyzed with the NCBI Gene database and the TissueEnrich webtool, which both utilized transcriptome data from the Mouse ENCODE Project to determine the tissue specificity of each protein. When mapping the isolated proteins to different murine tissues, we found that the proteomic landscape of the EVs was most highly enriched for the placenta by a fold change of 3 and with a statistically significant p-value of 10^{-29} (Fig. 9A). From a total of 1,446 proteins, 129 were elevated in the placenta while 15

exhibited expression patterns specifically restricted to this reproductive tissue. Upon further analysis, the proteins exclusively expressed in the placenta were also found to be characteristic markers of various placental cell types (Fig. 9B). For example, Prl3d1was reported as a common parietal trophoblast giant cell marker while Ctsj was associated with trophoblasts found within the labyrinthine layer (Nakajima et al., 2000; Simmons et al., 2008). Overall, through the discovery of numerous placenta-specific proteins via tissue enrichment analysis, we were able to validate that the samples contained EVs that were derived from a placental source. Additionally, by identifying some of these proteins as distinctive markers for various cell types within the placenta, we were able to gain insight into the cellular origins of our EVs as well to further confirm the presence of a strong placenta-specific signature.

A.

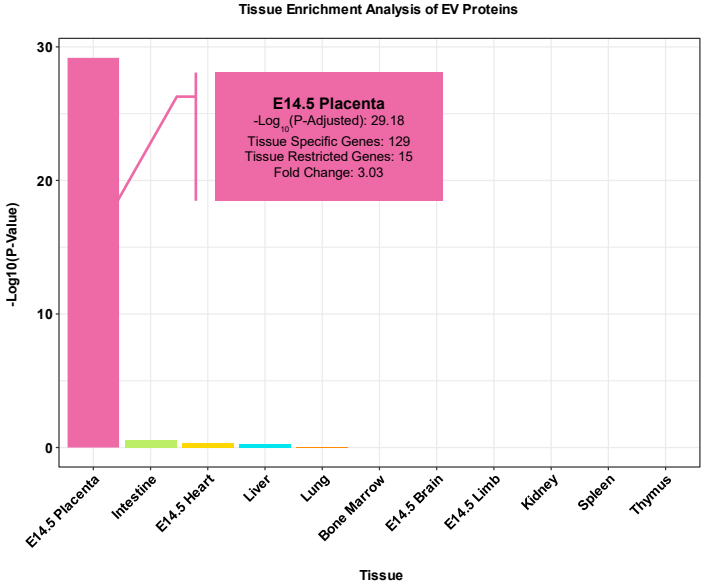

B.

Protein	Placental Cell Type
Prl2b1	S-TGC, SpT [1,2]
Prl2c2-5	SpA-TGC, C-TGC, P-TGC [1,2,3]
Prl3b1	P-TGC, SpT, S-TGC, C-TGC [1,2,3]
Prl3d1	P-TGC [1,2,3]
Prl4a1	P-TGC, SpA-TGC [1,2]
Prl7a1	P-TGC, SpT [2]
Prl7d1	P-TGC, SpA-TGC, C-TGC, SpT, GlyT, S-TGC [2]
Gzmd/e/f/g	GlyT, uNK, decidua [4,5]
Psg22	TGC [6]
Ctsj	Labyrinth trophoblast cells [7]

Figure 9. The proteome of the collected EVs exhibits a placenta-specific tissue signature: (A) Bar graph comparing the enrichment score of proteins from the *Nodal* CTL (N=4) and KO (N=4) EV samples across 11 different mouse tissues. The enrichment score is expressed on a -Log_{10}(p-value) scale where the p-value was calculated using the hypergeometric test and adjusted using the Benjamini & Hochberg correction procedure. (B) Table listing proteins from the EV samples that are exclusively found in the placenta and the placental cell types where they are most highly expressed. References are indicated as follows: [1](Simmons, 2014), [2](Simmons et al., 2008), [3](Simmons et al., 2007), [4](Sferruzzi-Perri et al., 2009), [5](Kaur et al., 2022), [6](Williams et al., 2015), [7](Nakajima et al., 2000).

3.2 Characterize the protein cargo of placental EVs derived from control and *Nodal* KO mice at mid-pregnancy

3.2.1 Placental EVs from Nodal KO females at mid-pregnancy differentially express proteins that are functionally involved in biological processes related to placentation compared to those from control females

Upon characterizing the proteome of the collected placental EVs, we also discovered that from a total of 1,446 proteins, 10 were exclusively expressed in EVs from the control mice while 14 were solely expressed in those derived from the *Nodal* KO females (Fig. 10A). When exploring the biological processes affiliated with these different proteins using GO analysis, we found that proteins exclusively found in the control EVs were interestingly enriched for GO terms which could be involved in placental development and function, such as "regulation of programmed cell death" (GO:0043067; p=0.0342), "response to oxidative stress" (GO:0006979; p=0.0105), "cellular anatomical entity morphogenesis" (GO:0032989; p=0.0339), and "oxygen transport" (GO:0015671; p=0.00409) (Fig. 10B). Likewise, proteins exclusively found in the *Nodal* KO EVs were enriched for GO terms such as "organic substance metabolic processes" (GO:0071704; p=0.0256), "anatomical structure development" (GO:0048856; p=0.0104), "system development" (GO:0048731; p=0.0157), and "angiogenesis" (GO:0001525; p=0.0194), which also allude to biological processes frequently linked to placentation (Fig. 10C).

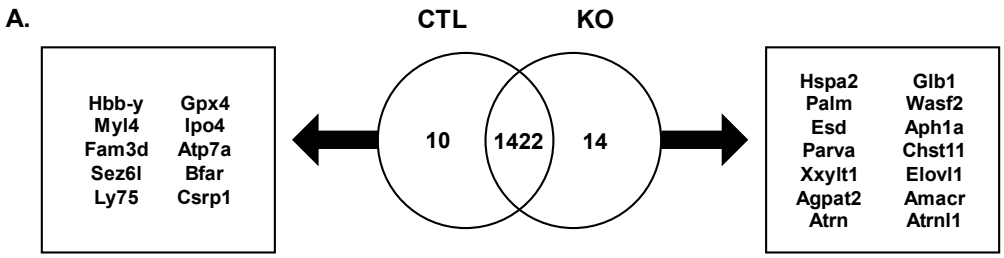

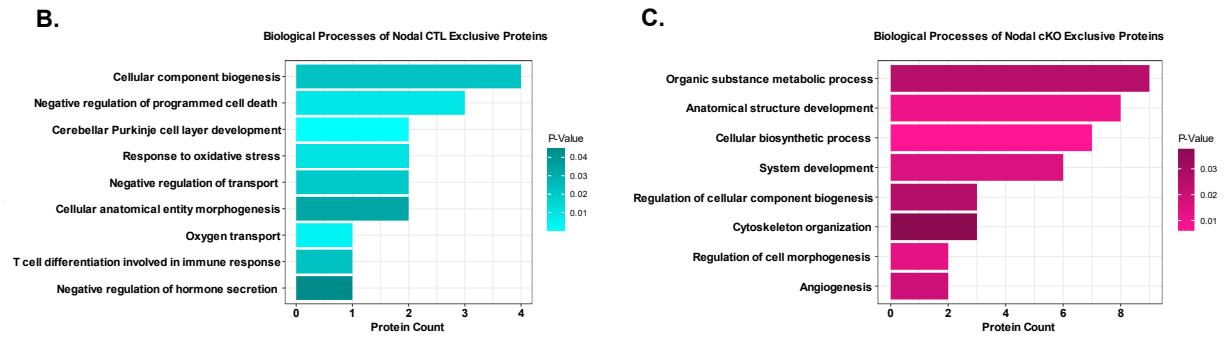

Figure 10. Comparing proteins exclusively found in EVs from CTL versus *Nodal* KO mice: (A) Venn diagram outlining the number of proteins found exclusively in EVs from the CTL (N=4) mice, *Nodal* KO (N=4) mice, or both strains. Proteins exclusively found in either the *Nodal* CTL or KO EVs are specified. (B) Placentation-related GO processes associated with the proteins exclusively found in the CTL EVs. (C) Placentation-related GO processes associated with the proteins exclusively found in the *Nodal* KO EVs. The bar colour in each GO graph indicates the enrichment score (p-value) for each biological process, although all specified terms have a p-value < 0.05. The top 3 GO terms based on protein count are also included to illustrate the relative enrichment of the placentation-related processes.

When expanding our analysis, 54 proteins were found to be significantly differentially expressed between the control and *Nodal* KO EVs with at least a fold-change of 1.5 and a p-value less than 0.05 (Fig. 11A). Of these proteins, 34 were upregulated in the *Nodal* KO EVs while 20 were downregulated. GO analysis revealed that many of the EV proteins differentially expressed between the two groups were associated with biological processes relevant for the morphological development of the placenta as well as its functional role as an endocrinological organ and modulator of the tissue's vasculature and immunological microenvironment. Specifically, we found that proteins upregulated in the *Nodal* KO EVs were enriched for GO terms pertaining to "anatomical structure development" (GO:0048856; p=0.00216), "blood vessel development" (GO:0001568; p=0.0115), "tissue remodeling" (GO:0048771; p=0.0172), "uterus development" (GO:0060065; p=0.0454), "response to progesterone" (GO:0032570; p=0.0305), "positive regulation of stem cell differentiation" (GO:2000738; p=0.0365), and "negative regulation of macrophage cytokine production" (GO:0010936; p=0.0214) (Fig. 11B). Similarly, proteins downregulated in the *Nodal* KO EVs were enriched for terms such as "animal organ development" (GO:0051049; p=0.00481), "regulation of anatomical structure size" (GO:0090066; p=0.0157), "blood vessel diameter maintenance" (GO:0097746; p=0.0129), "progesterone metabolic process" (GO:0042448; p=0.0154), and "negative regulation of cytokine production" (GO:0002719; p=0.0314) (Fig. 11C). Overall, our findings not only

highlighted distinct differences between the proteome of the EVs from the *Nodal* KO mice compared to the controls, but we found that the proteomic differences observed at mid-pregnancy are functionally involved in processes that mediate some of the major morphological and physiological changes that occur during placentation. This demonstrated that disturbances in placentation or related processes could be detected by cargo changes within our murine EVs at the protein level, further emphasizing their ability to potentially offer acute insight into the maternal-fetal interface.

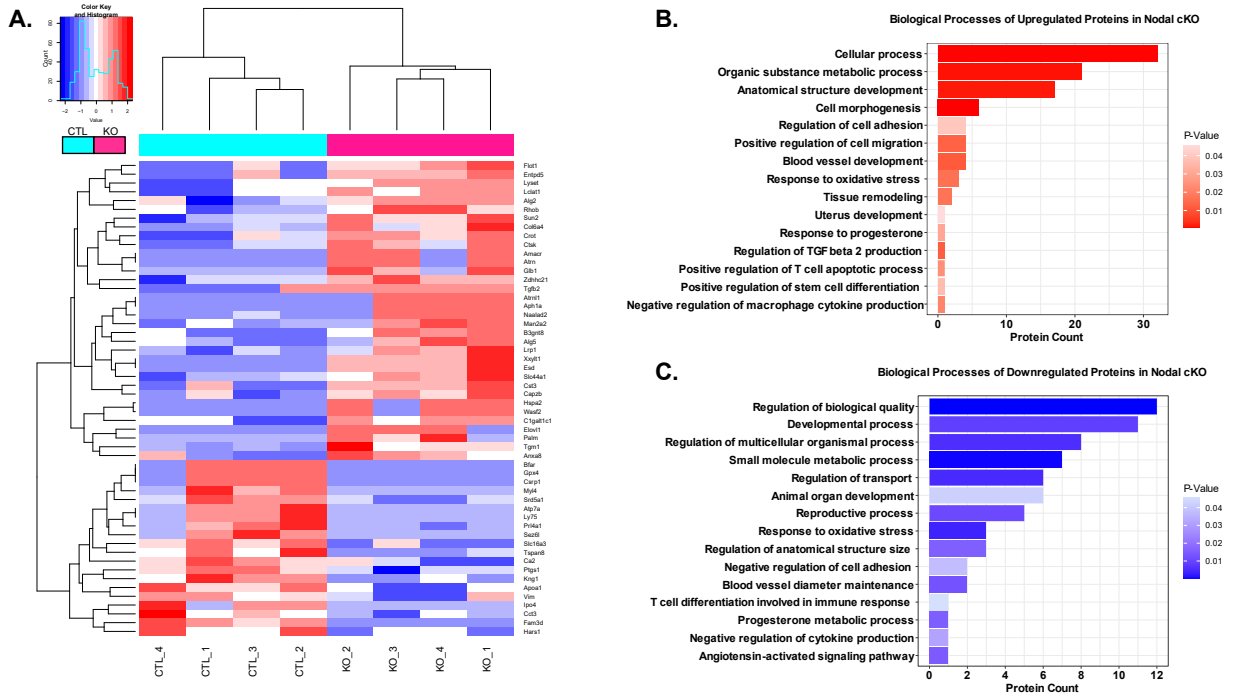

Figure 11. Comparing the expression and biological functions of EV proteins differentially expressed between the CTL and *Nodal* KO mice: (A) Heatmap displaying the expression and hierarchical clustering of proteins differentially expressed between the *Nodal* CTL (N=4) and KO (N=4) EV samples with a fold-change > 1.5 and a p-value < 0.05. Proteins were clustered using the Euclidean distance metric and complete linkage agglomeration method. Colour key denotes z-score normalized peptide counts where blue to red indicates low to high protein expression levels respectively. (B) Placentation-related GO biological processes associated with the proteins upregulated in the *Nodal* KO EVs. (C) Placentation-related GO biological processes associated with the proteins downregulated in the *Nodal* KO EVs. The bar colour in each GO graph indicates the enrichment score (p-value) for each biological process listed, although all have a p-value < 0.05. The top 3 GO terms based on protein count are also included for both bar graphs to illustrate the relative enrichment of the placentation-related processes compared to others implicated by the proteins differentially expressed in the *Nodal* KO EVs.

3.2.2 EV proteins that are differentially expressed between the two mouse strains are implicated in pathological phenotypes that are also observed in the Nodal KO females

To determine the phenotypic implications of the differentially expressed EV proteins between the *Nodal* control and KO mice, we mapped these proteins against the Mammalian Phenotype Ontology database. Some interesting phenotypic terms that were enriched in this analysis included “abnormal vascular development” (MP:0000259; p=0.00896), “abnormal extraembryonic tissue physiology” (MP:0004264; p=0.05), “abnormal leukocyte migration” (MP:0003156; p=0.034), “embryonic lethality between somite formation and embryo turning” (MP:0006206; p=0.0127), “increased susceptibility to weight loss” (MP:0010180; p=0.0314), and “abnormal pregnancy” (MP:0009661; p=0.0484) (Fig. 12A). These terms were particularly notable because they were consistent with many of the phenotypes observed in our *Nodal* KO females (Park et al., 2012a; M. R. Rana, 2022; unpublished data). As with the GO analysis, this validated the competency with which these nanoparticles could detect placental abnormalities and further highlighted how the EVs could demonstrate this ability in a more macroscopic manner as well to better understand the placenta in a pathologically meaningful way. In fact, additional analysis using the Disease Ontology database revealed that several of the differentially expressed EV proteins actually mapped to human diseases, such as “pre-eclampsia” (DOID:10591; p=0.0110), “pregnancy-induced hypertension” (DOID:9001650; p=0.0111), “proteinuria” (DOID:576; p=0.0253), “inflammation” (DOID:9005372; p=0.0483), and “vasculitis” (DOID:865; p=0.0173) (Fig. 12B), which emphasized their potential as biological indicators for real pregnancy complications and other relevant comorbidities.

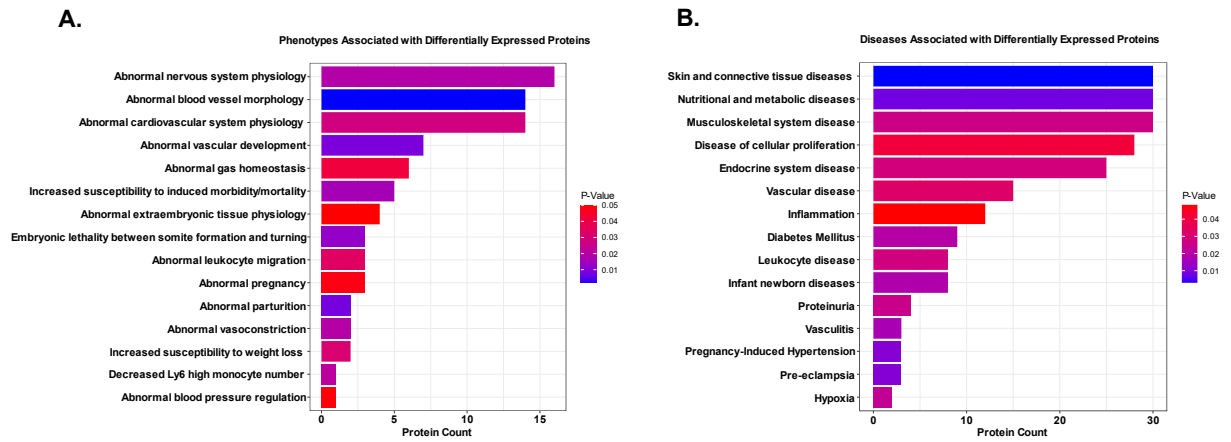

Figure 12. Phenotypes and diseases associated with the differentially expressed EV proteins: (A) Placental phenotypes associated with the proteins differentially expressed between the EVs from the *Nodal* CTL (N=4) and KO (N=4) mice. (B) Pregnancy-related complications associated with the EV proteins differentially expressed between the *Nodal* CTL and KO mice. The bar colour in each graph indicates the enrichment score (p-value) for each phenotype or disease term, although all have a p-value < 0.05. The top 3 phenotypes or diseases based on protein count are also included to illustrate the relative enrichment of the terms of interest compared to others associated with the differentially expressed EV proteins.

3.2.3 Select EV proteins that are differentially expressed between the Nodal CTL and KO mice exhibit strong potential as biomarkers for human placental complications

Because we ultimately hoped to utilize the obtained cargo data to put forth prospective biomarkers for various placental complications, we had to first determine whether each protein had previously established roles in related processes. To do this, a systematic literature review was performed for each EV protein differentially expressed between the control and *Nodal* KO mice. Additionally, several RNA-seq and microarray datasets of placental samples derived from patients with reproductive complications were analyzed to inquire whether the proposed biomarker candidates were previously found to be dysregulated under pathological conditions in humans as well. We identified 7 proteins which were reported to be directly involved in placentation and other related processes that could contribute to the pathophysiology of adverse reproductive outcomes (Fig. 13). Examples of their characterized roles included promoting trophoblast invasion and differentiation, controlling decidualization, upregulating angiogenesis, and modulating tissue immune responses (Fitzgerald et al., 2023; Liang et al., 2018; Z. Liu et al., 2023; Zhu et al., 2022). Because these proteins were functionally implicated in processes also

dysregulated in the *Nodal* KO mice, they were selected as the top biomarker candidates for the described placental abnormalities. Furthermore, in addition to some novel candidates, 4 of the selected proteins were previously found to be differentially expressed in placental samples from patients with pregnancy complications (Ackerman et al., 2023; Mistry et al., 2010; Verma et al., 2019). Although these previous studies analyzed term human placentas, the dysregulated expression of these proteins in the EVs from our *Nodal* KO mice at D10.5 as well reinforced their diagnostic potential as biomarkers capable of detecting pathological complications earlier during mid-pregnancy.

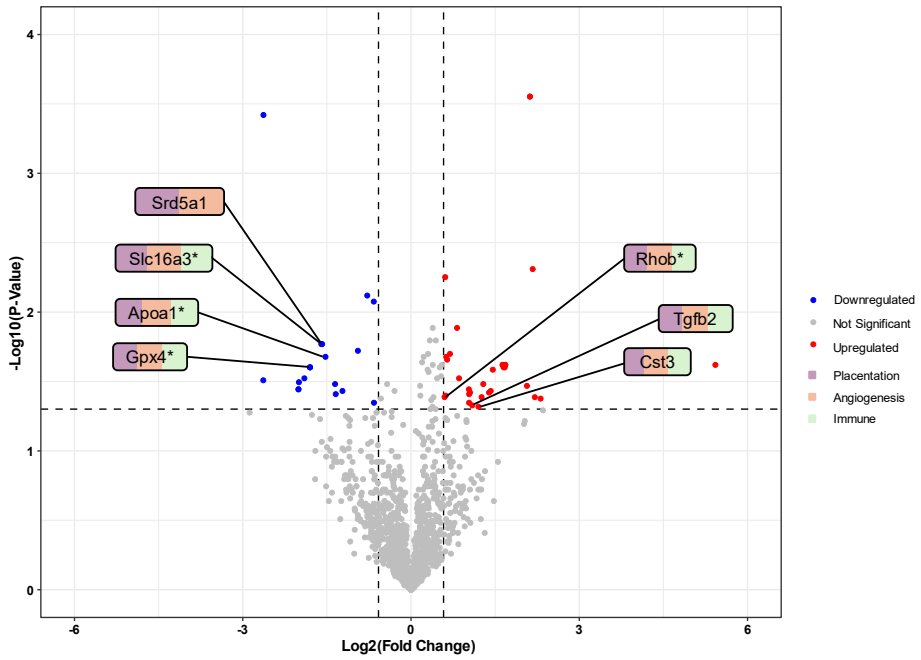

Figure 13. Top pregnancy complication biomarker candidates from placental EV proteins: Volcano plot illustrating the expression distribution of proteins from the *Nodal* CTL (N=4) and KO (N=4) EV samples. Proteins significantly downregulated in the *Nodal* KOs with a fold-change > 1.5 and a p-value < 0.05 are indicated in blue while those significantly upregulated are indicated in red. The top proteins of interest based on previously reported roles in pregnancy-related processes are specified. Proteins highlighted in purple, orange, or green have implicated roles in placental development, angiogenesis, or immune processes respectively. * denotes proteins that have been found to be differentially expressed in placental samples from patients with pregnancy pathologies in at least two separate transcriptome datasets or studies.

3.3 Characterize the miRNA cargo of placental EVs derived from control and *Nodal* KO mice at mid-pregnancy

3.3.1 Placental EVs from Nodal KO females at mid-pregnancy differentially express miRNAs that target genes functionally involved in biological processes related to placentation compared to those from control females

Along with proteins, the small RNA cargo of the isolated EVs was analyzed through miRNA-Seq. We found a total of 625 miRNAs of which 30 were exclusively expressed in EVs from the control mice while 20 were exclusive to the EVs from the *Nodal* KO females (Fig. 14A). When looking into the genes targeted by the miRNAs exclusive to the *Nodal* CTL and KO EVs, we found that 391 genes were targeted by the CTL exclusive EV miRNAs, 188 by the *Nodal* KO exclusive EV miRNAs, and 91 by both. Through GO analysis, we found that genes targeted by the CTL exclusive EV miRNAs were primarily involved in biological processes related to embryonic development as some of the top enriched terms included “pattern specification process” (GO:0007389; p=0.0193), “morphogenesis of embryonic epithelium” (GO:0016331; p=0.0356), and “ectoderm development” (GO:0007398; p=0.0193) (Fig. 14B). Some of the targeted genes were also found to be enriched in terms related to placental development and function as well, such as “positive regulation of angiogenesis” (GO:0045766; p=0.00983) and “hormone transport” (GO:0009914; p=0.0244). Meanwhile, the target genes of the EV miRNAs exclusive to the *Nodal* KO females were more extensively associated with placentation-related processes as many of the enriched GO terms included those such as “organ growth” (GO:0035265; p=0.0000493), “hormone secretion” (GO:0046879; p=0.0348), “cytokine production involved in immune response” (GO:0002367; p=0.00661), “glucose import” (GO:0046323; p=0.00139), “placenta development” (GO:0001890; p=0.0447), “maternal process involved in female pregnancy” (GO:0060135; p=0.0155), and “negative regulation of sprouting angiogenesis” (GO:1903671; p=0.0464) (Fig. 14C).

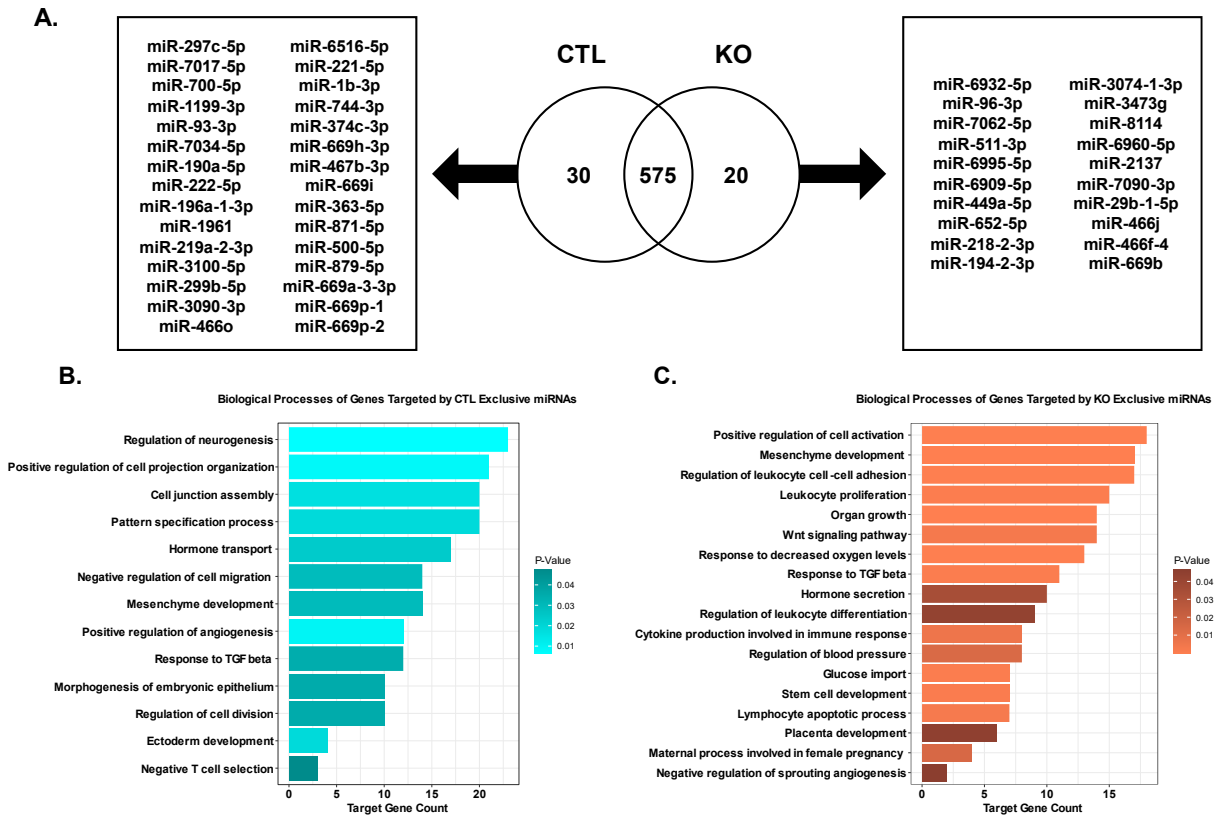

Figure 14. Comparing miRNAs exclusively found in EVs from the CTL versus *Nodal* KO mice: (A) Venn diagram outlining the number of miRNAs found exclusively in EVs from the CTL mice (N=3), *Nodal* KO mice (N=3), or both strains. miRNAs exclusively found in either the *Nodal* CTL or KO EVs are specified. (B) Placentation-related GO biological processes associated with the target genes of the miRNAs exclusively found in the CTL EVs. (C) Placentation-related GO biological processes associated with the target genes of the miRNAs exclusively found in the *Nodal* KO EVs. The bar colour for the GO graphs indicates the enrichment score (p-value) for each biological process, although all listed terms have a p-value < 0.05. The top 3 GO terms based on target gene count are included for each graph to illustrate the relative enrichment of the placentation-associated processes.

16 miRNAs were found to be significantly differentially expressed between the control and *Nodal* KO EVs with at least a $\log_2$ fold-change of 1.5 and a p-value less than 0.05 (Fig. 15A). Among the differentially expressed miRNAs, 6 were upregulated in the *Nodal* KO EVs while 10 were downregulated. These miRNAs targeted a total of 1094 genes where 497 were specifically targeted by the upregulated EV miRNAs, 511 by the downregulated miRNAs, and 86 by both. GO analysis of the target genes revealed that the differentially expressed miRNAs between the two groups were associated with various biological processes related to placental development and function. Target genes of miRNAs upregulated in the *Nodal* KO EVs were

linked to terms such as “developmental growth involved in morphogenesis” (GO:0060560; p=0.0000324), “placenta development” (GO:0001890; p=0.045), “hormone secretion” (GO:0046879; p=0.00911), “positive regulation of glucose import” (GO:0046326; p=0.014), “leukocyte proliferation” (GO:0070661; p=0.0245), and “negative regulation of cytokine production” (GO:0001818; p=0.0111) (Fig. 15B), which indicated how the upregulated EV miRNAs most likely impacted the morphological development placenta as well as its role as an endocrine organ, nutrient transporter, and immunomodulator of the maternal-fetal interface. Additionally, the enrichment of GO terms such as “canonical NFκB signal transduction” (GO:0007249; p=0.000173), “TGFβ receptor signaling pathway” (GO:0007179; p=0.00108), “positive regulation of Wnt signaling pathway” (GO:0030177; p=0.000594), and “EGFR signaling pathway” (GO:0007173; p=0.000824) reinforced the functional implications of these miRNAs as many of the specified molecular pathways have established roles in the aforementioned biological processes (Ariyakumar et al., 2021; Haider et al., 2022; Q. Li et al., 2007; Nishitani et al., 2023). Similar terms such as “reproductive system development” (GO:0061458; p=0.0302), “Wnt signaling pathway” (GO:0016055; p=0.00297), or “response to glucose” (GO:0009749; p=0.0224) were also enriched with the EV miRNAs downregulated in the *Nodal* KO mice (Fig. 15C). However, the downregulated miRNAs were found to be more extensively associated with processes concerning the formation and physiology of the placental vasculature as some of the top enriched GO terms for these miRNAs included “endothelial cell proliferation” (GO:0001935; p=0.00967), “endothelial cell differentiation” (GO:0045446; p=0.000696), and “response to decreased oxygen levels” (GO:0036293; p=0.00454). Overall, like with its protein cargo, the enrichment of these terms revealed the ability of the EVs to detect disturbances in placentation-related processes through changes in their miRNA transcriptome.

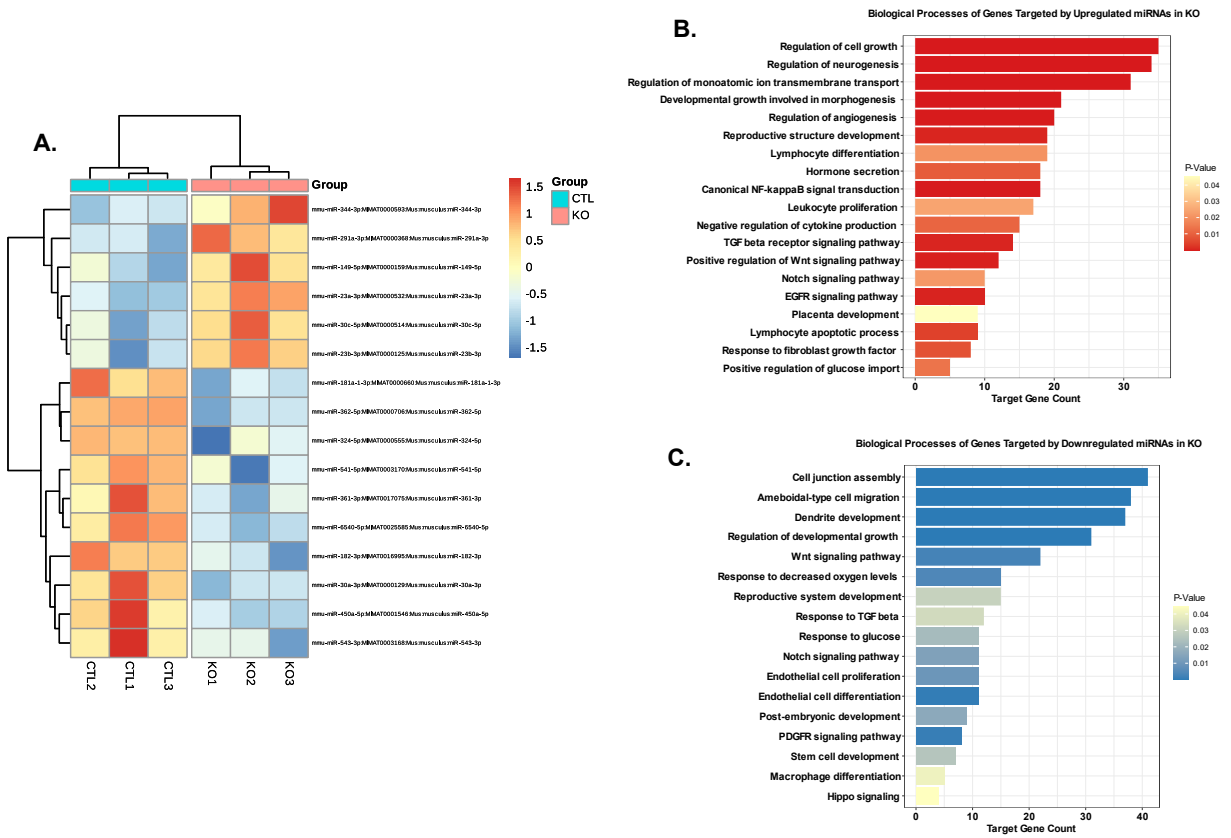

Figure 15. Comparing the expression and biological functions of EV miRNAs differentially expressed between the CTL and *Nodal* KO mice: (A) Heatmap displaying the expression and hierarchical clustering of miRNAs differentially expressed between the *Nodal* CTL (N=3) and KO (N=3) EV samples with a $\log_2$(fold-change) > 1.5 and a p-value < 0.05. Clustering was based on correlation distance and the complete linkage agglomeration method. Colour key denotes VST transformed transcript counts where blue to red indicates low to high expression levels respectively. (B) Placentation-related GO biological processes associated with the target genes of miRNAs upregulated in the *Nodal* KO EVs. (C) Placentation-related GO biological processes associated with target genes of miRNAs downregulated in the *Nodal* KO EVs. The bar colour in each GO graph indicates the enrichment score (p-value) for each biological process, although all have a p-value < 0.05. The top 3 terms based on target gene count are also included to illustrate the relative enrichment of the placentation-associated processes.

3.3.2 EV miRNAs that are differentially expressed between the two groups are implicated in pathological phenotypes that are also observed in the Nodal KO females

When mapping the target genes of the differentially expressed miRNAs against the Mammalian Phenotype Ontology database, we found numerous interesting terms that matched the phenotypes observed in the *Nodal* KO mice at mid-pregnancy (Park et al., 2012a; M. R.

Rana, 2022; unpublished data). Some of these terms included “decreased embryo size” (MP:0001698; p=0.000000365), “abnormal placenta morphology” (MP:0001711; p=0.0303), “abnormal placenta physiology” (MP:0010038; p=0.00902), “abnormal placenta vasculature” (MP:0003231; p=0.011), and “reduced female fertility” (MP:0001923; p=0.0178) (Fig. 16A). Additionally, when mapping the target genes of the differentially expressed miRNAs against the Disease Ontology database we found that they were associated with comorbidities related to placental dysfunction, such as “vascular disease” (DOID:178; p=0.0000603), “autoimmune disease” (DOID:417; p=0.0474), “hypertension” (DOID:10763; p=0.00495), “growth disorders” (DOID:9006257; p=0.0398), “placenta disease” (DOID:780; p=0.0199), and “embryo loss” (DOID:9004994; p=0.00803) (Fig. 16B). As with the protein cargo, these findings supported the potential of EV miRNAs as prospective biomarkers for pregnancy complications. Furthermore, by bioinformatically mapping to phenotypes actually observed in the *Nodal* KO females, we were able to highlight the relative accuracy with which these EV miRNAs could detect placental abnormalities and other pathological outcomes as well.

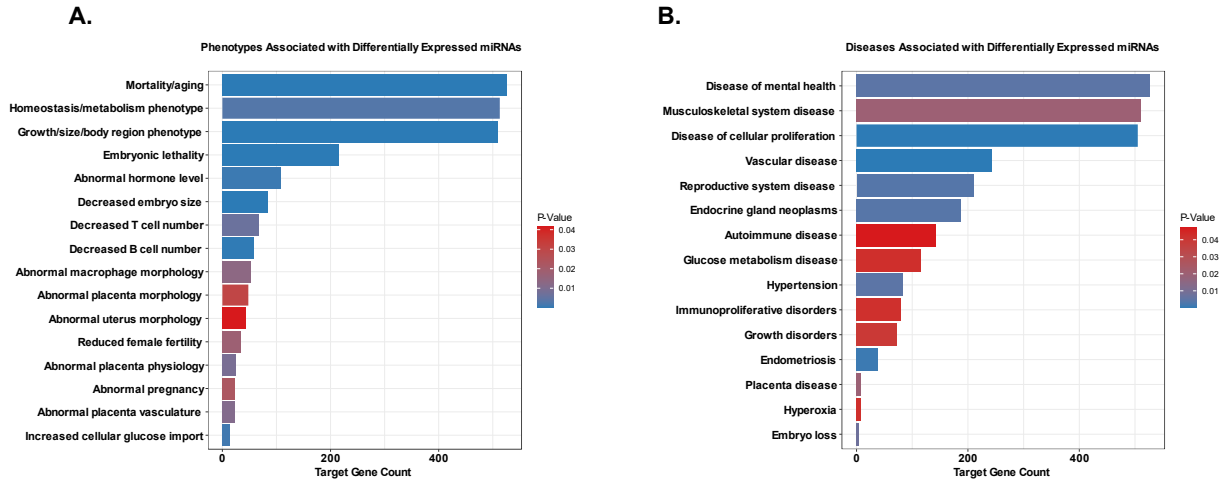

Figure 16. Phenotypes and diseases associated with the differentially expressed EV miRNAs: (A) Placental phenotypes associated with the miRNAs differentially expressed between the EVs from *Nodal* CTL (N=3) and KO (N=3) mice. (B) Pregnancy-related complications associated with the miRNAs differentially expressed between the EVs from *Nodal* CTL and KO mice. The bar colour in each graph indicates the enrichment score (p-value) for each phenotype or disease term, although they all have a p-value < 0.05. The top 3 phenotypes or diseases based on target gene count are also included to illustrate the relative enrichment of the terms of interest compared to others associated with the differentially expressed EV miRNAs.

3.3.3 Select EV miRNAs that are differentially expressed between the Nodal CTL and KO mice exhibit strong potential as biomarkers for human placental complications

To determine which differentially expressed miRNAs could serve as pregnancy complication biomarkers, we performed a literature review of the target genes associated with the top ontology terms of interest. We discovered 45 target genes which were directly involved in placentation or related processes, such as trophoblast invasion and differentiation, decidualization, angiogenesis, and inflammation (Fig. 16) (Jaykumar et al., 2022; Kamei et al., 2002; Large et al., 2014; Ma et al., 2014; Xue et al., 2019). Interestingly, these genes interacted with the same 6 miRNAs, and thus were selected as the top biomarker candidates because of their established roles in processes known to be dysregulated in various reproductive complications as well as the *Nodal* KO mice. When analyzing published studies on placental samples derived from patients with pregnancy complications, we found that only miR-30c-5p was previously found to be differentially expressed in patients with preeclampsia and IUGR (Timofeeva et al., 2021). In addition to the introduction of 5 other differentially expressed miRNAs as novel biomarker candidates, the dysregulated expression of miR-30c-5p in human patients further validated its diagnostic potential and clinical applicability as a biological indicator for mid-pregnancy pathological phenotypes.

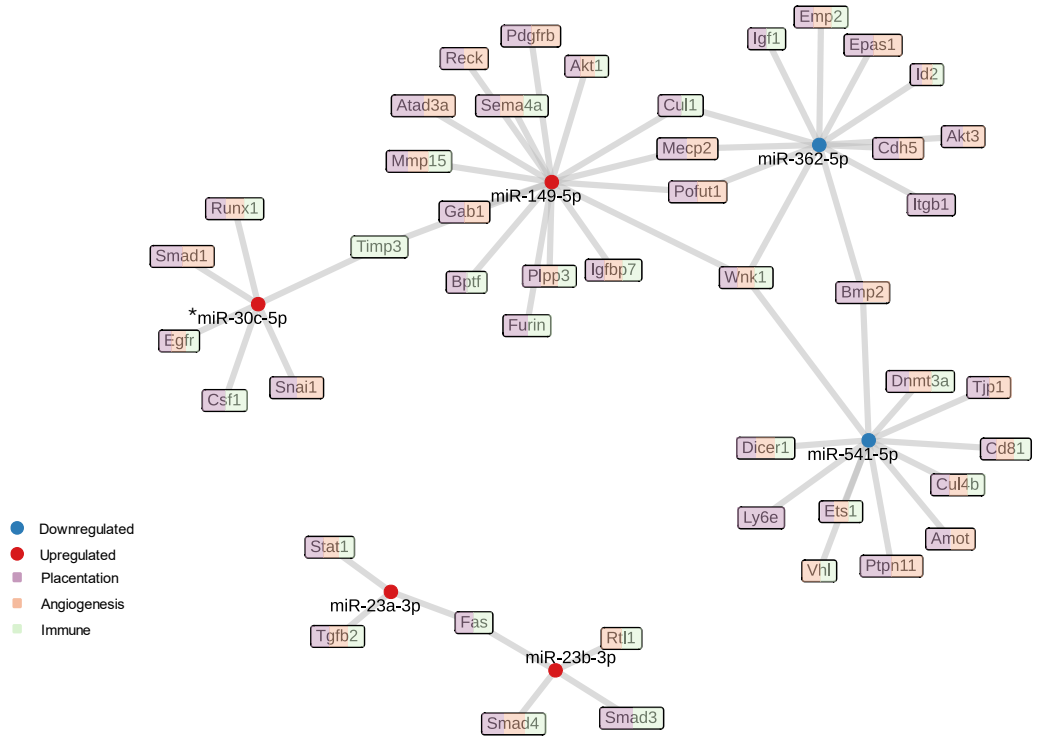

Figure 17. Top pregnancy complication biomarker candidates from placental EV miRNAs: Network schematic illustrating the top EV miRNAs of interest and their target genes. miRNAs indicated by red nodes are significantly upregulated while those indicated by blue nodes are downregulated in the *Nodal* KO EVs. Target genes highlighted in purple, orange, or green have established roles in placental development, angiogenesis, or immune processes respectively. * denotes miRNAs that were also differentially expressed in placental samples from patients with pregnancy complications.

4. DISCUSSION

The presented thesis aimed to explore the feasibility of placenta-derived EVs as potential biological indicators for pathological reproductive phenotypes at mid-gestation. Previous studies have demonstrated the mechanistic role EVs could play in the pathophysiology of placental complications from impairing trophoblast differentiation to generating a proinflammatory tissue environment detrimental towards fetal survival (Kohli et al., 2016; Markmeyer et al., 2021). Because of this, several groups have attempted to characterize EVs from pathologically implicated placentas for potential biomarkers that could explain and later be used to detect the phenotypic changes observed in patients with reproductive complications. For example, in one study, decreased levels of endothelial nitric oxide synthase in EVs from perfused preeclamptic placentas was identified as a biological indicator for preeclampsia due to the enzyme's implicated role as a mediator for the vasoconstriction and hypertension commonly seen in patients (Motta-Mejia et al., 2017). In a different study, the upregulated expression of miR-9-5p in syncytiotrophoblast EVs from preeclamptic placentas was believed to be another prospective biomarker for preeclampsia because of its implicated role in angiogenesis, which is largely known to be dysregulated in pathological cases (Awoyemi et al., 2024). While previous studies have assessed the potential of placental EVs as carriers for prospective pregnancy complication biomarkers, many of the proposed candidates were characterized with EVs from term placentas or trophoblast cell lines, which were limited in their ability to faithfully recapitulate the exact tissue environment responsible for the pathologies in question. Uncertainty regarding the accuracy of the characterized biomarker candidates thus led us to re-assess whether placental EVs could provide insight into the pathological changes that occur during a complicated pregnancy using our *Nodal* KO mice, which modelled clear placental phenotypes while also offering easy access to the developing placental tissue to address the aforementioned concerns regarding the sample source.

We hypothesized that the placental abnormalities in our *Nodal* KO mice would alter the EVs from the maternal-fetal interface in a manner that was indicative of the pathological phenotypes observed at mid-pregnancy. To explore this hypothesis, we compared the protein and miRNA cargo of placental EVs from our control and *Nodal* KO mice at D10.5, which was the initial timepoint when many of the dysregulated phenotypes were seen to manifest (Park et al., 2012b; M. R. Rana, 2022). Through our analysis, we found numerous distinct differences in the

proteome and miRNA transcriptome of the EVs between the control and *Nodal* KO mice. One of the first major differences was the existence of EV cargo components which were exclusive to each strain. In the EVs from the control mice, we discovered that there were 10 proteins and 30 miRNAs which were exclusively found in these nanoparticles. GO analysis revealed that the control-exclusive EV proteins were associated with various biological processes related to placental function, such as oxygen transport and hormone secretion, while the miRNAs were primarily linked to processes concerning embryonic development (Goplerud & Delivoria-Papadopoulos, 1985; Gude et al., 2004). Alternatively, 14 proteins and 20 miRNAs were exclusively found in the EVs from the *Nodal* KO mice. Proteins exclusive to the *Nodal* KO EVs were implicated in processes related to the morphological and vasculature development of the placenta while the miRNAs were additionally linked to functional processes commonly associated with the tissue, such as glucose import, regulation of blood pressure, and modulation of the tissue's immunological landscape (Gude et al., 2004; Mizutani & Tomoda, 1996; Smith et al., 2021). The enriched GO terms for the strain-exclusive cargo components indicated differences and thus the dysregulation of various processes involved in placental development and function between the control and *Nodal* KO mice. However, because the biological differences between the two strains could not be accounted for based on the presence or absence of certain cargo components alone, proteins and miRNAs differentially expressed between the EVs from the control and *Nodal* KO mice were analyzed as well.

GO analysis of the cargo components differentially expressed between the control and *Nodal* KO mice revealed the significant enrichment of multiple terms relevant to placentation. According to our analysis, some of the enriched terms associated with the differentially expressed cargo components suggested that the formation and morphogenesis of the placenta itself was dysregulated in the *Nodal* KO mice. For example, target genes of the miRNAs upregulated in the *Nodal* KO EVs were associated with GO terms like "placental development" as well as molecular pathways that mediate trophoblast and decidual stromal cell proliferation and differentiation, such as the "TGFβ receptor signaling pathway", "Wnt signaling pathway", and "EGFR signaling pathway" (Haider et al., 2022; Q. Li et al., 2007; Nishitani et al., 2023). Because miRNAs generally act as transcriptional repressors, the genes and placentation processes targeted by the upregulated miRNAs were predicted to be downregulated in the *Nodal* KO females (Jonas & Izaurralde, 2015). Supporting the analysis findings, placentation was also

significantly impaired in the *Nodal* KO dams at mid-pregnancy as the maternal decidual portion of the placenta was found to be severely diminished due to reduced cellular proliferation by gestational D10.5 (Park et al., 2012b; M. R. Rana, 2022). Additionally, while not observed until D14.5 of gestation, the fetal portions of the placentas from these mice were also notably thinner than the controls, which reinforced the validity of the dysfunctional placental phenotypes proposed by the GO terms enriched by the upregulated miRNAs in the *Nodal* KO EVs (M. R. Rana, 2022).

Another facet of the placenta that was predicted to be impacted by the differentially expressed EV cargo components was the development and physiology of its vasculature, which is essential for mediating resource exchange for fetal development and maternal-fetal communication for general pregnancy maintenance (Simmons, 2014). Among the implicated EV cargo components, proteins with functional roles in "blood vessel development" were upregulated while miRNAs that reduce the expression of genes that mediate "endothelial cell proliferation" and "endothelial cell differentiation" were downregulated. Interestingly, while the placental labyrinth of our *Nodal* KO females displayed a decreased density in maternal blood spaces, the upregulated angiogenesis implicated by the EVs was more consistent the compensatory expansion of fetal blood vessels also observed in the placentas of these mice (M. R. Rana, 2022). Given that the proportion of fetal tissue was higher in our sample source, the enrichment of proangiogenic EVs from the placental layer responsible for the development of the fetal vasculature network was expected. Regarding the physiology of the placental vasculature, proteins that mediate "blood vessel diameter maintenance" and miRNAs that target genes involved the tissue's "response to decreased oxygen levels" were downregulated, which suggested the dysfunctional vasoconstriction of placental blood vessels and elevated tissue hypoxia respectively. Complementary to the phenotypes proposed by the enriched GO terms, the *Nodal* KO females exhibited an increased expression of the vasoconstrictor gene *Edn1* as well as decreased levels of *Tac2*, which was a factor previously found to be downregulated upon exposure to hypoxic environmental conditions (Kiowski et al., 1991; Page et al., 2006; unpublished data).

The maintenance of an immunosuppressive placental microenvironment is essential for promoting maternal tolerance towards fetal antigens to minimize the physiological stresses exposed to the developing fetus during pregnancy (Ding et al., 2022; Smith et al., 2021).

However, in the placental EVs from our *Nodal* KO mice, we observed the dysregulated expression of numerous factors that mediate this immunological process at both the protein and miRNA level. For example, downregulated proteins and target genes of upregulated miRNAs in the *Nodal* KO EVs were associated with GO terms such as "negative regulation of cytokine production" and "leukocyte proliferation", while upregulated EV proteins were linked to the "negative regulation of macrophage cytokine production". Previously, we found the increased expression of several proinflammatory factors in the reproductive tract of the *Nodal* mutant dams from mid- to late pregnancy, such as *Il-1α*, *Il-1β*, and *Mx1*, which was consistent with the enriched GO term that predicted an increased production of cytokines in our mice (Ayash et al., 2020; unpublished data). Additionally, when characterizing the immune cell profiles of the *Nodal* KO females at gestational day 10.5, we had noted a depletion of some major anti-inflammatory mediators, such as neutrophils and M2 macrophages, within the maternal-fetal interface (Bouhlel et al., 2007; Marwick et al., 2018; unpublished data). Because these cellular phenotypes complemented the decreased expansion of leukocytes and macrophage activity anticipated by our GO analysis, we further demonstrated the competency with which placental EVs could correctly detect the immunological abnormalities exhibited by the *Nodal* KO mice.

Finally, we found that the differentially expressed EV cargo components were strongly associated with processes related to fetal growth. EV proteins downregulated in the *Nodal* KO mice were predicted to compromise the "regulation of anatomical structure size" while miRNAs upregulated in the *Nodal* KO dams were believed to similarly impede "developmental growth involved in morphogenesis" and metabolic pathways essential for providing nutrients for fetal growth, such as "glucose import" (Marconi et al., 1996). The impaired fetal growth and development that was implicated by our GO analysis was supported by the corresponding decrease in embryo size seen in the *Nodal* KO females at mid-pregnancy (Park et al., 2012b; M. R. Rana, 2022). Again, this indicated the consistency between the dysregulated phenotypes suggested by the placental EVs with those actually observed in our mouse model, emphasizing the relative accuracy with which these nanoparticles could detect placental abnormalities. In fact, when comparing our data against a phenotype ontology database, we found that many of the enriched terms, such as "decreased embryo size", "abnormal placenta morphology", "abnormal placenta physiology", and "abnormal vascular development", also mapped to the same implicated and observed phenotypes, which further demonstrated this ability.

Based on their exhibited phenotypes, the *Nodal* KO mice have been characterized as disease models for various pregnancy complications, such as preeclampsia and IUGR. Complementary to this, we found that many of the differentially expressed EV proteins and miRNAs derived from these mice bioinformatically mapped to human diseases, such as "pre-eclampsia", "hypertension", "growth disorders", "embryo loss", and "inflammation". This not only reinforced the validity of our disease model but highlighted the potential for the isolated EVs to be analyzed and harnessed as prospective disease biomarkers for diagnostic purposes as well. Upon performing a literature review of the differentially expressed EV proteins and miRNAs, we found several strong biomarker candidates with demonstrated functional roles in placentation and related physiological processes, which were also dysregulated in the *Nodal* KO mice. For example, Cst3 was an upregulated EV protein that had previously been found to attenuate the decidualization of endometrial stromal cells and induce VEGF-mediated angiogenesis when overexpressed, which was consistent with pathological phenotypes observed in the decidual and fetal labyrinth layers of the placentas from the *Nodal* KO mice respectively (Fitzgerald et al., 2023; M. R. Rana, 2022; Zou et al., 2017). Meanwhile, Slc16a3 was a downregulated protein in the *Nodal* KO EVs that had been characterized as a marker for syncytiotrophoblast layer II cells, a major lactate transporter necessary for embryonic growth, and an immunosuppressive factor that increased the production of anti-inflammatory cytokines in previous studies (Moreau et al., 2014; Vrooman et al., 2020; Zhu et al., 2022). The effects of downregulating Slc16a3 were also similarly reflected by the impaired fetal growth and proinflammatory placental environment seen in the *Nodal* KO females at mid-pregnancy (M. R. Rana, 2022; unpublished data). Among the differentially expressed miRNA cargo, we found several miRNAs that recurrently interacted with target genes associated with pregnancy-related processes. miR-149-5p was an upregulated miRNA in the *Nodal* KO EVs that targeted genes like *Akt1*. Previous studies revealed that the decreased expression of *Akt1* reduced placental and fetal weight in rats as well as the proliferation and tube formation of endothelial cells, which was consistent with the thinner fetal tissues, reduced embryo size, and diminished maternal vasculature observed in the *Nodal* KO females respectively (Feng et al., 2012; Kent et al., 2012; M. R. Rana, 2022). Another miRNA that was upregulated in the *Nodal* KO females was miR-30c-5p, which was known to target genes like *Egfr*. Previously, the downregulation of *Egfr* was found to compromise the proliferation and differentiation of endometrial stromal cells in mice

and significantly reduce the release of antiangiogenic factor sFlt-1 from primary cytotrophoblasts (Hastie et al., 2019; Large et al., 2014). This was complementary to the reduced decidual area and increased density of fetal blood vessels seen in the placentas of the *Nodal* KO mice (Park et al., 2012a; M. R. Rana, 2022). While increased characterization of the aforementioned EV cargo molecules is needed to confirm how they mediate the pathological phenotypes observed in the *Nodal* KO mice, the presented findings supported their strength as potential biological indicators of placental dysfunction. Moreover, by discovering that several of our highlighted EV proteins and miRNAs of interest, such as Slc16a3 and miR-30c-5p, were differentially expressed in term placentas from human patients with pregnancy complications, we were able to further reaffirm the relevance and clinical applicability of the presented candidates as prospective diagnostic biomarkers as well (Ackerman et al., 2023; Awamleh et al., 2019; Blair et al., 2013; Timofeeva et al., 2021).

Although the presented study yielded many interesting findings, some of our conclusions were challenged by experimental limitations. One of the first major limitations of the study was that the term enrichment analysis was primarily performed using the over-representation analysis (ORA) method, which determined pertinent biological terms based on the number of associated proteins or target genes alone (S. Zhang et al., 2010). While ideal for identifying relevant proteins or genes of interest from a specified list, such as those differentially expressed between the control and *Nodal* KO mice, the ORA method failed to provide insight on how the directionality or magnitude of the expression change for a given factor could impact implicated biological processes. For example, among the differentially expressed proteins in the *Nodal* KO mice, we found many that were associated with “blood vessel development”. However, we were unable to completely ascertain how the up- or downregulation of these proteins specifically affected angiogenesis without further literature review. Because of this, the correlations between the dysregulated biological processes proposed by our GO analysis with those observed in the mice were recognized to be made with a certain degree of assumption and uncertainty, which questioned the accuracy with which the EVs could detect pathological signs.

Another limitation was in regard to the validity and clinical translatability of the presented biomarker candidates in the study. Although each of the delineated candidates had previously demonstrated roles in processes involved in placentation, the studies that characterized these functional roles utilized various research models, tissues, and experimental

conditions. This made it difficult to ascertain whether the implicated candidates truly exerted a pathophysiological effect in our particular mouse model, which challenged their validity as potential biomarkers for placental complications. Additionally, because we had yet to confirm whether the proposed candidates were present and differentially expressed in placental EVs from patient plasma samples, we were unable to determine the likelihood of the selected proteins and miRNAs being developed into a minimally invasive diagnostic strategy as well.

While there were some notable limitations that challenged our findings, additional experiments could be performed to address many of the listed experimental concerns. For example, to confront the concerns regarding the biological relevance of the implicated EV proteins and miRNAs in the *Nodal* KO mice, we propose that functional studies either ablating or overexpressing these EV cargo components be conducted in mice or appropriate cell lines. This would not only validate the proposed roles of the selected biomarker candidates but would also further elucidate the pathophysiological mechanisms underlying the observed phenotypes in our mouse model. Additionally, we suggest that placental EVs from the plasma of patients with pregnancy complications be investigated using highly sensitive quantitative techniques, such as ELISA or qPCR, to assess the translatability our work as well as the diagnostic capabilities of the proposed biomarker candidates under real clinical contexts.

Overall, the presented findings strongly supported our hypothesis which stated that placental abnormalities caused by dysfunctional maternal Nodal signaling in the mouse would alter the EVs from the placenta in a manner that was indicative of the pathological phenotypes observed at mid-pregnancy. By characterizing the cargo of the collected placental EVs, we found that the dysregulated biological processes implicated in our analysis correspondingly matched the pathological phenotypes observed in the *Nodal* KO females. This demonstrated how placental abnormalities could be detected with reasonable accuracy through the analysis of these nanoparticles, which highlighted their potential as pathological indicators. In fact, we were able to identify several EV proteins and miRNAs that could be further explored as prospective biomarkers for complications like preeclampsia or IUGR, which were modelled by our *Nodal* KO mice as well. Ultimately, through our findings, we made significant progress in exploring the feasibility of a transformative diagnostic strategy that not only offered novel insight into the maternal-fetal interface, but an opportunity for disease detection that was proactive, accurate, and minimally invasive in its approach.

5. CONCLUSION

In conclusion, this thesis demonstrated the ability by which placental EVs could detect the presence of morphological and physiological abnormalities at the maternal-fetal interface in the mouse through molecular changes in their cargo composition. Using a previously established mouse model for pregnancy complications that ablated the *Nodal* gene in the maternal reproductive tract, we found that EVs derived from the placentas of these mice possessed a distinct proteomic and miRNA profile that differed from the control females. Cargo components differentially expressed between the two strains were associated with the dysregulation of various biological processes, such as organ growth and development, angiogenesis, metabolism, hypoxia, hormone secretion, cytokine production, and immune cell regulation. Interestingly, our analysis complemented the dysfunctional phenotypes observed in the *Nodal* KO mice, which emphasized the capability of the EVs to provide acute insight into the placental tissue environment. We also discovered that EV proteins and miRNAs differentially expressed between the control and *Nodal* KO females bioinformatically mapped to human pathologies, such as pre-eclampsia, hypertension, growth disorders, and inflammation, which reinforced the validity of our mice as a reproductive disease model that could be further investigated for prospective pathological biomarkers. In fact, subsequent analysis of individual cargo components revealed several biomarker candidates with reported roles in processes closely linked with the pathophysiology of prevalent placental complications as well as the phenotypes observed in the *Nodal* KO mice. For the first time, by characterizing the placental EVs from our *Nodal* KO mice at mid-pregnancy, we were able to assess the feasibility and relative accuracy with which EVs could indicate early pathological signs of placental dysfunction close to the time of symptomatic onset. Although further studies are needed to verify the clinical translatability of our work, the presented findings highlight the potential for these nanoparticles to be adapted into a novel diagnostic approach that addresses the limitations of currently available options to improve maternal-fetal health prospects for patients with high-risk pregnancy complications worldwide.

REFERENCES

Abbot, P., & Rokas, A. (2017). Mammalian pregnancy. *Current Biology : CB*, *27*(4), R127–R128. https://doi.org/10.1016/j.cub.2016.10.046

Ackerman, W. E. 4th, Buhimschi, C. S., Brown, T. L., Zhao, G., Summerfield, T. L., & Buhimschi, I. A. (2023). Transcriptomics-Based Subphenotyping of the Human Placenta Enabled by Weighted Correlation Network Analysis in Early-Onset Preeclampsia With and Without Fetal Growth Restriction. *Hypertension (Dallas, Tex. : 1979)*, *80*(6), 1363–1374. https://doi.org/10.1161/HYPERTENSIONAHA.122.20807

Aguilera, N., Salas-Pérez, F., Ortíz, M., Álvarez, D., Echiburú, B., & Maliqueo, M. (2022). Rodent models in placental research. Implications for fetal origins of adult disease. *Animal Reproduction*, *19*(1), e20210134. https://doi.org/10.1590/1984-3143-AR2021-0134

Altei, W. F., Pachane, B. C., dos Santos, P. K., Ribeiro, L. N. M., Sung, B. H., Weaver, A. M., & Selistre-de-Araújo, H. S. (2020). Inhibition of αvβ3 integrin impairs adhesion and uptake of tumor-derived small extracellular vesicles. *Cell Communication and Signaling*, *18*(1), 158. https://doi.org/10.1186/s12964-020-00630-w

Ariyakumar, G., Morris, J. M., McKelvey, K. J., Ashton, A. W., & McCracken, S. A. (2021). NF-κB regulation in maternal immunity during normal and IUGR pregnancies. *Scientific Reports*, *11*(1), 20971. https://doi.org/10.1038/s41598-021-00430-3

Armengaud, J. B., Yzydorczyk, C., Siddeek, B., Peyter, A. C., & Simeoni, U. (2021). Intrauterine growth restriction: Clinical consequences on health and disease at adulthood. *48th Conference of the European Teratology Society (ETS)*, *99*, 168–176. https://doi.org/10.1016/j.reprotox.2020.10.005

Awamleh, Z., Gloor, G. B., & Han, V. K. M. (2019). Placental microRNAs in pregnancies with early onset intrauterine growth restriction and preeclampsia: Potential impact on gene expression and pathophysiology. *BMC Medical Genomics*, *12*(1), 91. https://doi.org/10.1186/s12920-019-0548-x

Awoyemi, T., Jiang, S., Rahbar, M., Logentherian, P., Collett, G., Zhang, W., Cribbs, A., Cerdeira, S., & Vatish, M. (2024). MicroRNA analysis of medium/large placenta extracellular vesicles in normal and preeclampsia pregnancies. *Frontiers in Cardiovascular Medicine*, *11*, 1371168. https://doi.org/10.3389/fcvm.2024.1371168

Ayash, T. A., Starr, L. M., & Dufort, D. (2020). Nodal is required to maintain the uterine environment in an anti-inflammatory state during pregnancy†. *Biology of Reproduction*, *102*(6), 1340–1350. https://doi.org/10.1093/biolre/ioaa037

Beck, S., Le Good, J. A., Guzman, M., Haim, N. B., Roy, K., Beermann, F., & Constam, D. B. (2002). Extraembryonic proteases regulate Nodal signalling during gastrulation. *Nature Cell Biology*, *4*(12), 981–985. https://doi.org/10.1038/ncb890

Bentwich, I., Avniel, A., Karov, Y., Aharonov, R., Gilad, S., Barad, O., Barzilai, A., Einat, P., Einav, U., Meiri, E., Sharon, E., Spector, Y., & Bentwich, Z. (2005). Identification of hundreds of conserved and nonconserved human microRNAs. *Nature Genetics*, *37*(7), 766–770. https://doi.org/10.1038/ng1590

Blair, J. D., Yuen, R. K. C., Lim, B. K., McFadden, D. E., von Dadelszen, P., & Robinson, W. P. (2013). Widespread DNA hypomethylation at gene enhancer regions in placentas associated with early-onset pre-eclampsia. *Molecular Human Reproduction*, *19*(10), 697–708. https://doi.org/10.1093/molehr/gat044

Bouhlel, M. A., Derudas, B., Rigamonti, E., Dièvart, R., Brozek, J., Haulon, S., Zawadzki, C., Jude, B., Torpier, G., Marx, N., Staels, B., & Chinetti-Gbaguidi, G. (2007). PPARgamma activation primes human monocytes into alternative M2 macrophages with anti-inflammatory properties. *Cell Metabolism*, *6*(2), 137–143. https://doi.org/10.1016/j.cmet.2007.06.010

Brennan, J., Norris, D. P., & Robertson, E. J. (2002). Nodal activity in the node governs left-right asymmetry. *Genes & Development*, *16*(18), 2339–2344. https://doi.org/10.1101/gad.1016202

Bryda, E. C. (2013). The Mighty Mouse: The impact of rodents on advances in biomedical research. *Missouri Medicine*, *110*(3), 207–211.

Burton, G. J., & Fowden, A. L. (2015). The placenta: A multifaceted, transient organ. *Philosophical Transactions of the Royal Society of London. Series B, Biological Sciences*, *370*(1663), 20140066. https://doi.org/10.1098/rstb.2014.0066

Chaemsaithong, P., Luewan, S., Taweevisit, M., Chiangjong, W., Pongchaikul, P., Thorner, P. S., Tongsong, T., & Chutipongtanate, S. (2023). Placenta-Derived Extracellular Vesicles in Pregnancy Complications and Prospects on a Liquid Biopsy for Hemoglobin Bart's

Disease. *International Journal of Molecular Sciences*, *24*(6). https://doi.org/10.3390/ijms24065658

Chen, X., Weisberg, E., Fridmacher, V., Watanabe, M., Naco, G., & Whitman, M. (1997). Smad4 and FAST-1 in the assembly of activin-responsive factor. *Nature*, *389*(6646), 85–89. https://doi.org/10.1038/38008

Christianson, H. C., Svensson, K. J., van Kuppevelt, T. H., Li, J.-P., & Belting, M. (2013). Cancer cell exosomes depend on cell-surface heparan sulfate proteoglycans for their internalization and functional activity. *Proceedings of the National Academy of Sciences of the United States of America*, *110*(43), 17380–17385. https://doi.org/10.1073/pnas.1304266110

Colombo, M., Moita, C., van Niel, G., Kowal, J., Vigneron, J., Benaroch, P., Manel, N., Moita, L. F., Théry, C., & Raposo, G. (2013). Analysis of ESCRT functions in exosome biogenesis, composition and secretion highlights the heterogeneity of extracellular vesicles. *Journal of Cell Science*, *126*(Pt 24), 5553–5565. https://doi.org/10.1242/jcs.128868

Conlon, F. L., Barth, K. S., & Robertson, E. J. (1991). A novel retrovirally induced embryonic lethal mutation in the mouse: Assessment of the developmental fate of embryonic stem cells homozygous for the 413.d proviral integration. *Development (Cambridge, England)*, *111*(4), 969–981. https://doi.org/10.1242/dev.111.4.969

Conlon, F. L., Lyons, K. M., Takaesu, N., Barth, K. S., Kispert, A., Herrmann, B., & Robertson, E. J. (1994). A primary requirement for nodal in the formation and maintenance of the primitive streak in the mouse. *Development (Cambridge, England)*, *120*(7), 1919–1928. https://doi.org/10.1242/dev.120.7.1919

Cooke, W. R., Jiang, P., Ji, L., Bai, J., Jones, G. D., Lo, Y. M. D., Redman, C., & Vatish, M. (2024). Differential 5'-tRNA Fragment Expression in Circulating Preeclampsia Syncytiotrophoblast Vesicles Drives Macrophage Inflammation. *Hypertension (Dallas, Tex. : 1979)*, *81*(4), 876–886. https://doi.org/10.1161/HYPERTENSIONAHA.123.22292

Crescitelli, R., Lässer, C., & Lötvall, J. (2021). Isolation and characterization of extracellular vesicle subpopulations from tissues. *Nature Protocols*, *16*(3), 1548–1580. https://doi.org/10.1038/s41596-020-00466-1

Cui, J., Chen, X., Lin, S., Li, L., Fan, J., Hou, H., & Li, P. (2020). MiR-101-containing extracellular vesicles bind to BRD4 and enhance proliferation and migration of trophoblasts in preeclampsia. *Stem Cell Research & Therapy*, *11*(1), 231. https://doi.org/10.1186/s13287-020-01720-9

Ding, J., Maxwell, A., Adzibolosu, N., Hu, A., You, Y., Liao, A., & Mor, G. (2022). Mechanisms of immune regulation by the placenta: Role of type I interferon and interferon-stimulated genes signaling during pregnancy. *Immunological Reviews*, *308*(1), 9–24. https://doi.org/10.1111/imr.13077

Evans, T. J., & Ganjam, V. K. (2011). Chapter 2—Reproductive anatomy and physiology. In R. C. Gupta (Ed.), *Reproductive and Developmental Toxicology* (pp. 7–32). Academic Press. https://doi.org/10.1016/B978-0-12-382032-7.10002-5

Favaro, R., Abrahamsohn, P. A., & Zorn, M. T. (2014). 11—Decidualization and Endometrial Extracellular Matrix Remodeling. In B. A. Croy, A. T. Yamada, F. J. DeMayo, & S. L. Adamson (Eds.), *The Guide to Investigation of Mouse Pregnancy* (pp. 125–142). Academic Press. https://doi.org/10.1016/B978-0-12-394445-0.00011-4

Feng, L., Liao, W.-X., Luo, Q., Zhang, H.-H., Wang, W., Zheng, J., & Chen, D.-B. (2012). Caveolin-1 orchestrates fibroblast growth factor 2 signaling control of angiogenesis in placental artery endothelial cell caveolae. *Journal of Cellular Physiology*, *227*(6), 2480–2491. https://doi.org/10.1002/jcp.22984

Fitzgerald, H. C., Kelleher, A. M., Ranjit, C., Schust, D. J., & Spencer, T. E. (2023). Basolateral secretions of human endometrial epithelial organoids impact stromal cell decidualization. *Molecular Human Reproduction*, *29*(4). https://doi.org/10.1093/molehr/gaad007

Fitzner, D., Schnaars, M., van Rossum, D., Krishnamoorthy, G., Dibaj, P., Bakhti, M., Regen, T., Hanisch, U.-K., & Simons, M. (2011). Selective transfer of exosomes from oligodendrocytes to microglia by macropinocytosis. *Journal of Cell Science*, *124*(Pt 3), 447–458. https://doi.org/10.1242/jcs.074088

Fox, J. E., Austin, C. D., Reynolds, C. C., & Steffen, P. K. (1991). Evidence that agonist-induced activation of calpain causes the shedding of procoagulant-containing microvesicles from the membrane of aggregating platelets. *The Journal of Biological Chemistry*, *266*(20), 13289–13295.

Ghadami, S., & Dellinger, K. (2023). The lipid composition of extracellular vesicles: Applications in diagnostics and therapeutic delivery. *Frontiers in Molecular Biosciences*, *10*, 1198044. https://doi.org/10.3389/fmolb.2023.1198044

Gills, J. J., Zhang, C., Abu-Asab, M. S., Castillo, S. S., Marceau, C., LoPiccolo, J., Kozikowski, A. P., Tsokos, M., Goldkorn, T., & Dennis, P. A. (2012). Ceramide mediates nanovesicle shedding and cell death in response to phosphatidylinositol ether lipid analogs and perifosine. *Cell Death & Disease*, *3*(7), e340–e340. https://doi.org/10.1038/cddis.2012.72

Goplerud, J. M., & Delivoria-Papadopoulos, M. (1985). Physiology of the placenta—Gas exchange. *Annals of Clinical and Laboratory Science*, *15*(4), 270–278.

Gude, N. M., Roberts, C. T., Kalionis, B., & King, R. G. (2004). Growth and function of the normal human placenta. *Thrombosis Research*, *114*(5–6), 397–407. https://doi.org/10.1016/j.thromres.2004.06.038

Haider, S., Lackner, A. I., Dietrich, B., Kunihs, V., Haslinger, P., Meinhardt, G., Maxian, T., Saleh, L., Fiala, C., Pollheimer, J., Latos, P. A., & Knöfler, M. (2022). Transforming growth factor-β signaling governs the differentiation program of extravillous trophoblasts in the developing human placenta. *Proceedings of the National Academy of Sciences of the United States of America*, *119*(28), e2120667119. https://doi.org/10.1073/pnas.2120667119

Hánělová, K., Raudenská, M., Masařík, M., & Balvan, J. (2024). Protein cargo in extracellular vesicles as the key mediator in the progression of cancer. *Cell Communication and Signaling*, *22*(1), 25. https://doi.org/10.1186/s12964-023-01408-6

Hastie, R., Brownfoot, F. C., Pritchard, N., Hannan, N. J., Cannon, P., Nguyen, V., Palmer, K., Beard, S., Tong, S., & Kaitu'u-Lino, T. J. (2019). EGFR (Epidermal Growth Factor Receptor) Signaling and the Mitochondria Regulate sFlt-1 (Soluble FMS-Like Tyrosine Kinase-1) Secretion. *Hypertension (Dallas, Tex. : 1979)*, *73*(3), 659–670. https://doi.org/10.1161/HYPERTENSIONAHA.118.12300

Hemberger, M., Hanna, C. W., & Dean, W. (2020). Mechanisms of early placental development in mouse and humans. *Nature Reviews Genetics*, *21*(1), 27–43. https://doi.org/10.1038/s41576-019-0169-4

Hessvik, N. P., & Llorente, A. (2018). Current knowledge on exosome biogenesis and release. *Cell Mol Life Sci*, *75*(2), 193–208. https://doi.org/10.1007/s00018-017-2595-9

Huppertz, B. (2008). Placental Origins of Preeclampsia. *Hypertension*, *51*(4), 970–975. https://doi.org/10.1161/HYPERTENSIONAHA.107.107607

Ibrahim, P., Denniston, R., Mitsuhashi, H., Yang, J., Fiori, L. M., Żurawek, D., Mechawar, N., Nagy, C., & Turecki, G. (2024). Profiling Small RNA From Brain Extracellular Vesicles in Individuals With Depression. *International Journal of Neuropsychopharmacology*, *27*(3), pyae013. https://doi.org/10.1093/ijnp/pyae013

Jahn, R., Cafiso, D. C., & Tamm, L. K. (2024). Mechanisms of SNARE proteins in membrane fusion. *Nature Reviews. Molecular Cell Biology*, *25*(2), 101–118. https://doi.org/10.1038/s41580-023-00668-x

Jain, A., & Tuteja, G. (2021). PlacentaCellEnrich: A tool to characterize gene sets using placenta cell-specific gene enrichment analysis. *Placenta*, *103*, 164–171. https://doi.org/10.1016/j.placenta.2020.10.029

Jain, V., Chodankar, R. R., Maybin, J. A., & Critchley, H. O. D. (2022). Uterine bleeding: How understanding endometrial physiology underpins menstrual health. *Nature Reviews Endocrinology*, *18*(5), 290–308. https://doi.org/10.1038/s41574-021-00629-4

Jaykumar, A. B., Plumber, S., Barry, D. M., Binns, D., Wichaidit, C., Grzemska, M., Earnest, S., Goldsmith, E. J., Cleaver, O., & Cobb, M. H. (2022). WNK1 collaborates with TGF-β in endothelial cell junction turnover and angiogenesis. *Proceedings of the National Academy of Sciences of the United States of America*, *119*(30), e2203743119. https://doi.org/10.1073/pnas.2203743119

Jonas, S., & Izaurralde, E. (2015). Towards a molecular understanding of microRNA-mediated gene silencing. *Nature Reviews Genetics*, *16*(7), 421–433. https://doi.org/10.1038/nrg3965

Jones, T. M., & Montero, F. J. (2022). Chorionic Villus Sampling. In *StatPearls [Internet]*. Treasure Island (FL): StatPearls Publishing. https://www.ncbi.nlm.nih.gov/books/NBK563301/

Joshi, B. S., de Beer, M. A., Giepmans, B. N. G., & Zuhorn, I. S. (2020). Endocytosis of Extracellular Vesicles and Release of Their Cargo from Endosomes. *ACS Nano*, *14*(4), 4444–4455. https://doi.org/10.1021/acsnano.9b10033

Kaltenegger, M., Kremser, J., Frewein, M. P. K., Ziherl, P., Bonthuis, D. J., & Pabst, G. (2021). Intrinsic lipid curvatures of mammalian plasma membrane outer leaflet lipids and

ceramides. *Biochimica et Biophysica Acta (BBA) - Biomembranes*, *1863*(11), 183709. https://doi.org/10.1016/j.bbamem.2021.183709

Kamei, T., Jones, S. R., Chapman, B. M., MCGonigle, K. L., Dai, G., & Soares, M. J. (2002). The phosphatidylinositol 3-kinase/Akt signaling pathway modulates the endocrine differentiation of trophoblast cells. *Molecular Endocrinology (Baltimore, Md.)*, *16*(7), 1469–1481. https://doi.org/10.1210/mend.16.7.0878

Katzmann, D. J., Babst, M., & Emr, S. D. (2001). Ubiquitin-Dependent Sorting into the Multivesicular Body Pathway Requires the Function of a Conserved Endosomal Protein Sorting Complex, ESCRT-I. *Cell*, *106*(2), 145–155. https://doi.org/10.1016/S0092-8674(01)00434-2

Kaur, G., Porter, C. B. M., Ashenberg, O., Lee, J., Riesenfeld, S. J., Hofree, M., Aggelakopoulou, M., Subramanian, A., Kuttikkatte, S. B., Attfield, K. E., Desel, C. A. E., Davies, J. L., Evans, H. G., Avraham-Davidi, I., Nguyen, L. T., Dionne, D. A., Neumann, A. E., Jensen, L. T., Barber, T. R., … Fugger, L. (2022). Mouse fetal growth restriction through parental and fetal immune gene variation and intercellular communications cascade. *Nature Communications*, *13*(1), 4398. https://doi.org/10.1038/s41467-022-32171-w

Keelan, J. A., Blumenstein, M., Helliwell, R. J. A., Sato, T. A., Marvin, K. W., & Mitchell, M. D. (2003). Cytokines, Prostaglandins and Parturition—A Review. *Placenta*, *24*, S33–S46. https://doi.org/10.1053/plac.2002.0948

Kent, L. N., Ohboshi, S., & Soares, M. J. (2012). Akt1 and insulin-like growth factor 2 (Igf2) regulate placentation and fetal/postnatal development. *The International Journal of Developmental Biology*, *56*(4), 255–261. https://doi.org/10.1387/ijdb.113407lk

Khan, B., Allah Yar, R., Khakwani, A. K., Karim, S., & Arslan Ali, H. (2022). Preeclampsia Incidence and Its Maternal and Neonatal Outcomes With Associated Risk Factors. *Cureus*, *14*(11), e31143. https://doi.org/10.7759/cureus.31143

Khatibzadeh, N., Spector, A. A., Brownell, W. E., & Anvari, B. (2013). Effects of plasma membrane cholesterol level and cytoskeleton F-actin on cell protrusion mechanics. *PloS One*, *8*(2), e57147. https://doi.org/10.1371/journal.pone.0057147

Kim, S.-M., & Kim, J.-S. (2017). A Review of Mechanisms of Implantation. *Development & Reproduction*, *21*(4), 351–359. https://doi.org/10.12717/DR.2017.21.4.351

Kiowski, W., Lüscher, T. F., Linder, L., & Bühler, F. R. (1991). Endothelin-1-induced vasoconstriction in humans. Reversal by calcium channel blockade but not by nitrovasodilators or endothelium-derived relaxing factor. *Circulation*, *83*(2), 469–475. https://doi.org/10.1161/01.cir.83.2.469

Kohli, S., Ranjan, S., Hoffmann, J., Kashif, M., Daniel, E. A., Al-Dabet, M. M., Bock, F., Nazir, S., Huebner, H., Mertens, P. R., Fischer, K.-D., Zenclussen, A. C., Offermanns, S., Aharon, A., Brenner, B., Shahzad, K., Ruebner, M., & Isermann, B. (2016). Maternal extracellular vesicles and platelets promote preeclampsia via inflammasome activation in trophoblasts. *Blood*, *128*(17), 2153–2164. https://doi.org/10.1182/blood-2016-03-705434

Kowal, J., Arras, G., Colombo, M., Jouve, M., Morath, J. P., Primdal-Bengtson, B., Dingli, F., Loew, D., Tkach, M., & Théry, C. (2016). Proteomic comparison defines novel markers to characterize heterogeneous populations of extracellular vesicle subtypes. *Proceedings of the National Academy of Sciences of the United States of America*, *113*(8), E968-977. https://doi.org/10.1073/pnas.1521230113

Kunadt, M., Eckermann, K., Stuendl, A., Gong, J., Russo, B., Strauss, K., Rai, S., Kügler, S., Falomir Lockhart, L., Schwalbe, M., Krumova, P., Oliveira, L. M. A., Bähr, M., Möbius, W., Levin, J., Giese, A., Kruse, N., Mollenhauer, B., Geiss-Friedlander, R., … Schneider, A. (2015). Extracellular vesicle sorting of α-Synuclein is regulated by sumoylation. *Acta Neuropathologica*, *129*(5), 695–713. https://doi.org/10.1007/s00401-015-1408-1

Kwok, Z. H., Wang, C., & Jin, Y. (2021). Extracellular Vesicle Transportation and Uptake by Recipient Cells: A Critical Process to Regulate Human Diseases. *Processes (Basel, Switzerland)*, *9*(2), 273. https://doi.org/10.3390/pr9020273

Large, M. J., Wetendorf, M., Lanz, R. B., Hartig, S. M., Creighton, C. J., Mancini, M. A., Kovanci, E., Lee, K.-F., Threadgill, D. W., Lydon, J. P., Jeong, J.-W., & DeMayo, F. J. (2014). The epidermal growth factor receptor critically regulates endometrial function during early pregnancy. *PLoS Genetics*, *10*(6), e1004451. https://doi.org/10.1371/journal.pgen.1004451

Larios, J., Mercier, V., Roux, A., & Gruenberg, J. (2020). ALIX- and ESCRT-III-dependent sorting of tetraspanins to exosomes. *The Journal of Cell Biology*, *219*(3). https://doi.org/10.1083/jcb.201904113

Le Good, J. A., Joubin, K., Giraldez, A. J., Ben-Haim, N., Beck, S., Chen, Y., Schier, A. F., & Constam, D. B. (2005). Nodal stability determines signaling range. *Current Biology : CB*, *15*(1), 31–36. https://doi.org/10.1016/j.cub.2004.12.062

Levine, L., Habertheuer, A., Ram, C., Korutla, L., Schwartz, N., Hu, R. W., Reddy, S., Freas, A., Zielinski, P. D., Harmon, J., Molugu, S. K., Parry, S., & Vallabhajosyula, P. (2020). Syncytiotrophoblast extracellular microvesicle profiles in maternal circulation for noninvasive diagnosis of preeclampsia. *Scientific Reports*, *10*(1), 6398. https://doi.org/10.1038/s41598-020-62193-7

Li, B., Antonyak, M. A., Zhang, J., & Cerione, R. A. (2012). RhoA triggers a specific signaling pathway that generates transforming microvesicles in cancer cells. *Oncogene*, *31*(45), 4740–4749. https://doi.org/10.1038/onc.2011.636

Li, Q., Kannan, A., Wang, W., Demayo, F. J., Taylor, R. N., Bagchi, M. K., & Bagchi, I. C. (2007). Bone morphogenetic protein 2 functions via a conserved signaling pathway involving Wnt4 to regulate uterine decidualization in the mouse and the human. *The Journal of Biological Chemistry*, *282*(43), 31725–31732. https://doi.org/10.1074/jbc.M704723200

Liang, H.-Z., Li, S.-F., Zhang, F., Wu, M.-Y., Li, C.-L., Song, J.-X., Lee, C., & Chen, H. (2018). Effect of Endothelial Microparticles Induced by Hypoxia on Migration and Angiogenesis of Human Umbilical Vein Endothelial Cells by Delivering MicroRNA-19b. *Chinese Medical Journal*, *131*(22), 2726–2733. https://doi.org/10.4103/0366-6999.245271

Liu, X., Fei, H., Yang, C., Wang, J., Zhu, X., Yang, A., Shi, Z., Jin, X., Yang, F., Wu, D., Jiang, L., & Zhang, S. (2022). Trophoblast-Derived Extracellular Vesicles Promote Preeclampsia by Regulating Macrophage Polarization. *Hypertension*, *79*(10), 2274–2287. https://doi.org/10.1161/hypertensionaha.122.19244

Liu, Z., Pei, J., Zhang, X., Wang, C., Tang, Y., Liu, H., Yu, Y., Luo, S., & Gu, W. (2023). APOA1 Is a Novel Marker for Preeclampsia. *International Journal of Molecular Sciences*, *24*(22). https://doi.org/10.3390/ijms242216363

Londin, E. R., Niemiec, J., & Sirotkin, H. I. (2005). Chordin, FGF signaling, and mesodermal factors cooperate in zebrafish neural induction. *Developmental Biology*, *279*(1), 1–19. https://doi.org/10.1016/j.ydbio.2004.11.016

Lu, C. C., & Robertson, E. J. (2004). Multiple roles for Nodal in the epiblast of the mouse embryo in the establishment of anterior-posterior patterning. *Developmental Biology*, *273*(1), 149–159. https://doi.org/10.1016/j.ydbio.2004.06.004

Ma, R., Gu, B., Gu, Y., Groome, L. J., & Wang, Y. (2014). Down-regulation of TIMP3 leads to increase in TACE expression and TNFα production by placental trophoblast cells. *American Journal of Reproductive Immunology (New York, N.Y. : 1989)*, *71*(5), 427–433. https://doi.org/10.1111/aji.12205

Mandruzzato, G., Antsaklis, A., Botet, F., Chervenak, F. A., Figueras, F., Grunebaum, A., Puerto, B., Skupski, D., & Stanojevic, M. (2008). *Intrauterine restriction (IUGR)*. *36*(4), 277–281. https://doi.org/10.1515/JPM.2008.050

Marconi, A. M., Paolini, C., Buscaglia, M., Zerbe, G., Battaglia, F. C., & Pardi, G. (1996). The impact of gestational age and fetal growth on the maternal-fetal glucose concentration difference. *Obstetrics and Gynecology*, *87*(6), 937–942. https://doi.org/10.1016/0029-7844(96)00048-8

Markmeyer, P., Lochmann, F., Singh, K. K., Gupta, A., Younis, R., Shahzad, K., Biemann, R., Huebner, H., Ruebner, M., Isermann, B., & Kohli, S. (2021). Procoagulant Extracellular Vesicles Alter Trophoblast Differentiation in Mice by a Thrombo-Inflammatory Mechanism. *International Journal of Molecular Sciences*, *22*(18). https://doi.org/10.3390/ijms22189873

Marwick, J. A., Mills, R., Kay, O., Michail, K., Stephen, J., Rossi, A. G., Dransfield, I., & Hirani, N. (2018). Neutrophils induce macrophage anti-inflammatory reprogramming by suppressing NF-κB activation. *Cell Death & Disease*, *9*(6), 665. https://doi.org/10.1038/s41419-018-0710-y

Meharwade, T., Joumier, L., Parisotto, M., Huynh, V., Lummertz da Rocha, E., & Malleshaiah, M. (2023). Cross-activation of FGF, NODAL, and WNT pathways constrains BMP-signaling-mediated induction of the totipotent state in mouse embryonic stem cells. *Cell Reports*, *42*(5), 112438. https://doi.org/10.1016/j.celrep.2023.112438

Mi, H., Muruganujan, A., Huang, X., Ebert, D., Mills, C., Guo, X., & Thomas, P. D. (2019). Protocol Update for large-scale genome and gene function analysis with the PANTHER classification system (v.14.0). *Nature Protocols*, *14*(3), 703–721. https://doi.org/10.1038/s41596-019-0128-8

Mistry, H. D., Kurlak, L. O., Williams, P. J., Ramsay, M. M., Symonds, M. E., & Broughton Pipkin, F. (2010). Differential expression and distribution of placental glutathione peroxidases 1, 3 and 4 in normal and preeclamptic pregnancy. *Placenta*, *31*(5), 401–408. https://doi.org/10.1016/j.placenta.2010.02.011

Mizutani, S., & Tomoda, Y. (1996). Effects of placental proteases on maternal and fetal blood pressure in normal pregnancy and preeclampsia. *American Journal of Hypertension*, *9*(6), 591–597. https://doi.org/10.1016/0895-7061(96)00016-7

Moreau, J. L. M., Artap, S. T., Shi, H., Chapman, G., Leone, G., Sparrow, D. B., & Dunwoodie, S. L. (2014). Cited2 is required in trophoblasts for correct placental capillary patterning. *Developmental Biology*, *392*(1), 62–79. https://doi.org/10.1016/j.ydbio.2014.04.023

Morelli, A. E., Larregina, A. T., Shufesky, W. J., Sullivan, M. L. G., Stolz, D. B., Papworth, G. D., Zahorchak, A. F., Logar, A. J., Wang, Z., Watkins, S. C., Falo, L. D. J., & Thomson, A. W. (2004). Endocytosis, intracellular sorting, and processing of exosomes by dendritic cells. *Blood*, *104*(10), 3257–3266. https://doi.org/10.1182/blood-2004-03-0824

Motta-Mejia, C., Kandzija, N., Zhang, W., Mhlomi, V., Cerdeira, A. S., Burdujan, A., Tannetta, D., Dragovic, R., Sargent, I. L., Redman, C. W., Kishore, U., & Vatish, M. (2017). Placental Vesicles Carry Active Endothelial Nitric Oxide Synthase and Their Activity is Reduced in Preeclampsia. *Hypertension (Dallas, Tex. : 1979)*, *70*(2), 372–381. https://doi.org/10.1161/HYPERTENSIONAHA.117.09321

Mukherjee, A., Soyal, S. M., Fernandez-Valdivia, R., Gehin, M., Chambon, P., Demayo, F. J., Lydon, J. P., & O'Malley, B. W. (2006). Steroid receptor coactivator 2 is critical for progesterone-dependent uterine function and mammary morphogenesis in the mouse. *Molecular and Cellular Biology*, *26*(17), 6571–6583. https://doi.org/10.1128/MCB.00654-06

Muralidharan-Chari, V., Clancy, J., Plou, C., Romao, M., Chavrier, P., Raposo, G., & D'Souza-Schorey, C. (2009). ARF6-regulated shedding of tumor cell-derived plasma membrane microvesicles. *Current Biology : CB*, *19*(22), 1875–1885. https://doi.org/10.1016/j.cub.2009.09.059

Murugesan, S., Hussey, H., Saravanakumar, L., Sinkey, R. G., Sturdivant, A. B., Powell, M. F., & Berkowitz, D. E. (2022). Extracellular Vesicles From Women With Severe Preeclampsia

Impair Vascular Endothelial Function. *Anesthesia and Analgesia*, *134*(4), 713–723. https://doi.org/10.1213/ANE.0000000000005812

Nakahara, A., Nair, S., Ormazabal, V., Elfeky, O., Garvey, C. E., Longo, S., & Salomon, C. (2020). Circulating Placental Extracellular Vesicles and Their Potential Roles During Pregnancy. *Ochsner Journal*, *20*(4), 439–445. https://doi.org/10.31486/toj.20.0049

Nakajima, A., Kataoka, K., Takata, Y., & Huh, N. H. (2000). Cathepsin-6, a novel cysteine proteinase showing homology with and co-localized expression with cathepsin J/P in the labyrinthine layer of mouse placenta. *The Biochemical Journal*, *349 Pt 3*(Pt 3), 689–692. https://doi.org/10.1042/bj3490689

National Center for Biotechnology Information. (2004). *NCBI Gene* [Dataset]. National Library of Medicine (US). Available from: https://www.ncbi.nlm.nih.gov/gene/

Nishitani, K., Hayakawa, K., & Tanaka, S. (2023). Epidermal growth factor represses differentiation of mouse trophoblast stem cells into spongiotrophoblast cells via epidermal growth factor receptor. *Biochemical and Biophysical Research Communications*, *657*, 100–107. https://doi.org/10.1016/j.bbrc.2023.03.059

Norwitz, E. R. (2006). Defective implantation and placentation: Laying the blueprint for pregnancy complications. *Reproductive Biomedicine Online*, *13*(4), 591–599. https://doi.org/10.1016/s1472-6483(10)60649-9

O'Brien, K., Breyne, K., Ughetto, S., Laurent, L. C., & Breakefield, X. O. (2020). RNA delivery by extracellular vesicles in mammalian cells and its applications. *Nature Reviews Molecular Cell Biology*, *21*(10), 585–606. https://doi.org/10.1038/s41580-020-0251-y

Ochoa-Bernal, M. A., & Fazleabas, A. T. (2020). Physiologic Events of Embryo Implantation and Decidualization in Human and Non-Human Primates. *International Journal of Molecular Sciences*, *21*(6). https://doi.org/10.3390/ijms21061973

Oka, Y., Tanaka, K., & Kawasaki, Y. (2023). A novel sorting signal for RNA packaging into small extracellular vesicles. *Scientific Reports*, *13*(1), 17436. https://doi.org/10.1038/s41598-023-44218-z

Ostrowski, M., Carmo, N. B., Krumeich, S., Fanget, I., Raposo, G., Savina, A., Moita, C. F., Schauer, K., Hume, A. N., Freitas, R. P., Goud, B., Benaroch, P., Hacohen, N., Fukuda, M., Desnos, C., Seabra, M. C., Darchen, F., Amigorena, S., Moita, L. F., & Thery, C.

(2010). Rab27a and Rab27b control different steps of the exosome secretion pathway. *Nature Cell Biology*, *12*(1), 19–30. https://doi.org/10.1038/ncb2000

Page, N. M., Dakour, J., & Morrish, D. W. (2006). Gene regulation of neurokinin B and its receptor NK3 in late pregnancy and pre-eclampsia. *Molecular Human Reproduction*, *12*(7), 427–433. https://doi.org/10.1093/molehr/gal025

Papageorgiou, I., Nicholls, P. K., Wang, F., Lackmann, M., Makanji, Y., Salamonsen, L. A., Robertson, D. M., & Harrison, C. A. (2009). Expression of nodal signalling components in cycling human endometrium and in endometrial cancer. *Reproductive Biology and Endocrinology : RB&E*, *7*, 122. https://doi.org/10.1186/1477-7827-7-122

Park, C. B., DeMayo, F. J., Lydon, J. P., & Dufort, D. (2012a). NODAL in the uterus is necessary for proper placental development and maintenance of pregnancy. *Biol Reprod*, *86*(6), 194. https://doi.org/10.1095/biolreprod.111.098277

Park, C. B., DeMayo, F. J., Lydon, J. P., & Dufort, D. (2012b). NODAL in the uterus is necessary for proper placental development and maintenance of pregnancy. *Biology of Reproduction*, *86*(6), 194. https://doi.org/10.1095/biolreprod.111.098277

Parolini, I., Federici, C., Raggi, C., Lugini, L., Palleschi, S., De Milito, A., Coscia, C., Iessi, E., Logozzi, M., Molinari, A., Colone, M., Tatti, M., Sargiacomo, M., & Fais, S. (2009). Microenvironmental pH is a key factor for exosome traffic in tumor cells. *The Journal of Biological Chemistry*, *284*(49), 34211–34222. https://doi.org/10.1074/jbc.M109.041152

Rana, M. R. (2022). *Investigating the effects of maternal Nodal on mouse placental development and vascularization during mid-pregnancy* [Master's thesis, McGill University]. https://escholarship.mcgill.ca/concern/theses/5d86p554f

Rana, S., Lemoine, E., Granger, J. P., & Karumanchi, S. A. (2019). Preeclampsia. *Circulation Research*, *124*(7), 1094–1112. https://doi.org/10.1161/CIRCRESAHA.118.313276

Reissmann, E., Jörnvall, H., Blokzijl, A., Andersson, O., Chang, C., Minchiotti, G., Persico, M. G., Ibáñez, C. F., & Brivanlou, A. H. (2001). The orphan receptor ALK7 and the Activin receptor ALK4 mediate signaling by Nodal proteins during vertebrate development. *Genes & Development*, *15*(15), 2010–2022. https://doi.org/10.1101/gad.201801

Rikkert, L. G., Nieuwland, R., Terstappen, L. W. M. M., & Coumans, F. A. W. (2019). Quality of extracellular vesicle images by transmission electron microscopy is operator and protocol

dependent. *Journal of Extracellular Vesicles*, *8*(1), 1555419. https://doi.org/10.1080/20013078.2018.1555419

Salomon, L. J., Sotiriadis, A., Wulff, C. B., Odibo, A., & Akolekar, R. (2019). Risk of miscarriage following amniocentesis or chorionic villus sampling: Systematic review of literature and updated meta-analysis. *Ultrasound in Obstetrics & Gynecology : The Official Journal of the International Society of Ultrasound in Obstetrics and Gynecology*, *54*(4), 442–451. https://doi.org/10.1002/uog.20353

Schier, A. F. (2009). Nodal morphogens. *Cold Spring Harbor Perspectives in Biology*, *1*(5), a003459. https://doi.org/10.1101/cshperspect.a003459

Sferruzzi-Perri, A. N., Macpherson, A. M., Roberts, C. T., & Robertson, S. A. (2009). Csf2 null mutation alters placental gene expression and trophoblast glycogen cell and giant cell abundance in mice. *Biology of Reproduction*, *81*(1), 207–221. https://doi.org/10.1095/biolreprod.108.073312

Sha, M., Zhang, S., Beejadhursing, R., Sun, Y., Qin, Y., Chen, S., & Li, W. (2023). Extracellular vesicles derived from hypoxic HTR-8/SVneo trophoblast inhibit endothelial cell functions through the miR-150-3p /CHPF pathway. *Placenta*, *138*, 21–32. https://doi.org/10.1016/j.placenta.2023.04.017

Sharma, D., Shastri, S., & Sharma, P. (2016). Intrauterine Growth Restriction: Antenatal and Postnatal Aspects. *Clinical Medicine Insights. Pediatrics*, *10*, 67–83. https://doi.org/10.4137/CMPed.S40070

Shen, M. M. (2007). Nodal signaling: Developmental roles and regulation. *Development (Cambridge, England)*, *134*(6), 1023–1034. https://doi.org/10.1242/dev.000166

Shi, S., Tan, Q., Liang, J., Cao, D., Wang, S., Liang, J., Chen, K., & Wang, Z. (2021). Placental trophoblast cell-derived exosomal microRNA-1290 promotes the interaction between endometrium and embryo by targeting LHX6. *Molecular Therapy Nucleic Acids*, *26*, 760–772. https://doi.org/10.1016/j.omtn.2021.09.009

Simmons, D. G. (2014). 12—Postimplantation Development of the Chorioallantoic Placenta. In B. A. Croy, A. T. Yamada, F. J. DeMayo, & S. L. Adamson (Eds.), *The Guide to Investigation of Mouse Pregnancy* (pp. 143–161). Academic Press. https://doi.org/10.1016/B978-0-12-394445-0.00012-6

Simmons, D. G., Fortier, A. L., & Cross, J. C. (2007). Diverse subtypes and developmental origins of trophoblast giant cells in the mouse placenta. *Developmental Biology*, *304*(2), 567–578. https://doi.org/10.1016/j.ydbio.2007.01.009

Simmons, D. G., Rawn, S., Davies, A., Hughes, M., & Cross, J. C. (2008). Spatial and temporal expression of the 23 murine Prolactin/Placental Lactogen-related genes is not associated with their position in the locus. *BMC Genomics*, *9*(1), 352. https://doi.org/10.1186/1471-2164-9-352

Sinha, S., Hoshino, D., Hong, N. H., Kirkbride, K. C., Grega-Larson, N. E., Seiki, M., Tyska, M. J., & Weaver, A. M. (2016). Cortactin promotes exosome secretion by controlling branched actin dynamics. *The Journal of Cell Biology*, *214*(2), 197–213. https://doi.org/10.1083/jcb.201601025

Smith, A. L., Bole Aldo, P., & Racicot, K. E. (2021). Chapter 17—Placental regulation of immune functions. In G. Mor (Ed.), *Reproductive Immunology* (pp. 335–348). Academic Press. https://doi.org/10.1016/B978-0-12-818508-7.00004-X

Soh, G. H., Pomreinke, A. P., & Müller, P. (2020). Integration of Nodal and BMP Signaling by Mutual Signaling Effector Antagonism. *Cell Reports*, *31*(1), 107487. https://doi.org/10.1016/j.celrep.2020.03.051

Soyal, S. M., Mukherjee, A., Lee, K. Y.-S., Li, J., Li, H., DeMayo, F. J., & Lydon, J. P. (2005). Cre-mediated recombination in cell lineages that express the progesterone receptor. *Genesis (New York, N.Y. : 2000)*, *41*(2), 58–66. https://doi.org/10.1002/gene.20098

Tanaka, C., Sakuma, R., Nakamura, T., Hamada, H., & Saijoh, Y. (2007). Long-range action of Nodal requires interaction with GDF1. *Genes & Development*, *21*(24), 3272–3282. https://doi.org/10.1101/gad.1623907

Teng, F., & Fussenegger, M. (2020). Shedding Light on Extracellular Vesicle Biogenesis and Bioengineering. *Advanced Science*, *8*, 2003505. https://doi.org/10.1002/advs.202003505

Thomas, P. D., Ebert, D., Muruganujan, A., Mushayahama, T., Albou, L.-P., & Mi, H. (2022). PANTHER: Making genome-scale phylogenetics accessible to all. *Protein Science*, *31*(1), 8–22. https://doi.org/10.1002/pro.4218

Tian, T., Zhu, Y.-L., Zhou, Y.-Y., Liang, G.-F., Wang, Y.-Y., Hu, F.-H., & Xiao, Z.-D. (2014). Exosome uptake through clathrin-mediated endocytosis and macropinocytosis and

mediating miR-21 delivery. *The Journal of Biological Chemistry*, *289*(32), 22258–22267. https://doi.org/10.1074/jbc.M114.588046

Timofeeva, A. V., Fedorov, I. S., Brzhozovskiy, A. G., Bugrova, A. E., Chagovets, V. V., Volochaeva, M. V., Starodubtseva, N. L., Frankevich, V. E., Nikolaev, E. N., Shmakov, R. G., & Sukhikh, G. T. (2021). miRNAs and Their Gene Targets-A Clue to Differentiate Pregnancies with Small for Gestational Age Newborns, Intrauterine Growth Restriction, and Preeclampsia. *Diagnostics (Basel, Switzerland)*, *11*(4). https://doi.org/10.3390/diagnostics11040729

Trajkovic, K., Hsu, C., Chiantia, S., Rajendran, L., Wenzel, D., Wieland, F., Schwille, P., Brügger, B., & Simons, M. (2008). Ceramide Triggers Budding of Exosome Vesicles into Multivesicular Endosomes. *Science*, *319*(5867), 1244–1247. https://doi.org/10.1126/science.1153124

Vallier, L., Alexander, M., & Pedersen, R. A. (2005). Activin/Nodal and FGF pathways cooperate to maintain pluripotency of human embryonic stem cells. *Journal of Cell Science*, *118*(Pt 19), 4495–4509. https://doi.org/10.1242/jcs.02553

van Niel, G., Charrin, S., Simoes, S., Romao, M., Rochin, L., Saftig, P., Marks, M. S., Rubinstein, E., & Raposo, G. (2011). The tetraspanin CD63 regulates ESCRT-independent and -dependent endosomal sorting during melanogenesis. *Developmental Cell*, *21*(4), 708–721. https://doi.org/10.1016/j.devcel.2011.08.019

van Niel, G., D'Angelo, G., & Raposo, G. (2018). Shedding light on the cell biology of extracellular vesicles. *Nature Reviews. Molecular Cell Biology*, *19*(4), 213–228. https://doi.org/10.1038/nrm.2017.125

Vedi, M., Nalabolu, H. S., Lin, C.-W., Hoffman, M. J., Smith, J. R., Brodie, K., De Pons, J. L., Demos, W. M., Gibson, A. C., Hayman, G. T., Hill, M. L., Kaldunski, M. L., Lamers, L., Laulederkind, S. J. F., Thorat, K., Thota, J., Tutaj, M., Tutaj, M. A., Wang, S.-J., … Kwitek, A. E. (2022). MOET: a web-based gene set enrichment tool at the Rat Genome Database for multiontology and multispecies analyses. *Genetics*, *220*(4). https://doi.org/10.1093/genetics/iyac005

Verma, P., Nair, R. R., Singh, S., Rajender, S., Khanna, A., Jha, R. K., & Singh, K. (2019). High Level of APOA1 in Blood and Maternal Fetal Interface Is Associated With Early

Miscarriage. *Reproductive Sciences (Thousand Oaks, Calif.)*, *26*(5), 649–656. https://doi.org/10.1177/1933719118783266

Villarroya-Beltri, C., Baixauli, F., Mittelbrunn, M., Fernández-Delgado, I., Torralba, D., Moreno-Gonzalo, O., Baldanta, S., Enrich, C., Guerra, S., & Sánchez-Madrid, F. (2016). ISGylation controls exosome secretion by promoting lysosomal degradation of MVB proteins. *Nature Communications*, *7*, 13588. https://doi.org/10.1038/ncomms13588

Villarroya-Beltri, C., Gutiérrez-Vázquez, C., Sánchez-Cabo, F., Pérez-Hernández, D., Vázquez, J., Martin-Cofreces, N., Martinez-Herrera, D. J., Pascual-Montano, A., Mittelbrunn, M., & Sánchez-Madrid, F. (2013). Sumoylated hnRNPA2B1 controls the sorting of miRNAs into exosomes through binding to specific motifs. *Nature Communications*, *4*, 2980. https://doi.org/10.1038/ncomms3980

Vrooman, L. A., Rhon-Calderon, E. A., Chao, O. Y., Nguyen, D. K., Narapareddy, L., Dahiya, A. K., Putt, M. E., Schultz, R. M., & Bartolomei, M. S. (2020). Assisted reproductive technologies induce temporally specific placental defects and the preeclampsia risk marker sFLT1 in mouse. *Development (Cambridge, England)*, *147*(11). https://doi.org/10.1242/dev.186551

Watson, E. D., & Cross, J. C. (2005). Development of structures and transport functions in the mouse placenta. *Physiology (Bethesda, Md.)*, *20*, 180–193. https://doi.org/10.1152/physiol.00001.2005

Welsh, J. A., Goberdhan, D. C. I., O'Driscoll, L., Buzas, E. I., Blenkiron, C., Bussolati, B., Cai, H., Di Vizio, D., Driedonks, T. A. P., Erdbrügger, U., Falcon-Perez, J. M., Fu, Q.-L., Hill, A. F., Lenassi, M., Lim, S. K., Mahoney, M. G., Mohanty, S., Möller, A., Nieuwland, R., … Witwer, K. W. (2024). Minimal information for studies of extracellular vesicles (MISEV2023): From basic to advanced approaches. *Journal of Extracellular Vesicles*, *13*(2), e12404. https://doi.org/10.1002/jev2.12404

Williams, J. M., Ball, M., Ward, A., & Moore, T. (2015). Psg22 expression in mouse trophoblast giant cells is associated with gene inversion and co-expression of antisense long non-coding RNAs. *Reproduction (Cambridge, England)*, *149*(1), 125–137. https://doi.org/10.1530/REP-14-0390

Wlizla, M., & Zorn, A. M. (2015). Chapter 13—Vertebrate Endoderm Formation. In S. A. Moody (Ed.), *Principles of Developmental Genetics (Second Edition)* (pp. 237–253). Academic Press. https://doi.org/10.1016/B978-0-12-405945-0.00013-2

Wu, N., Cernysiov, V., Davidson, D., Song, H., Tang, J., Luo, S., Lu, Y., Qian, J., Gyurova, I. E., Waggoner, S. N., Trinh, V. Q.-H., Cayrol, R., Sugiura, A., McBride, H. M., Daudelin, J.-F., Labrecque, N., & Veillette, A. (2020). Critical Role of Lipid Scramblase TMEM16F in Phosphatidylserine Exposure and Repair of Plasma Membrane after Pore Formation. *Cell Reports*, *30*(4), 1129-1140.e5. https://doi.org/10.1016/j.celrep.2019.12.066

Xue, F., Yang, J., Li, Q., & Zhou, H. (2019). Down-regulation of microRNA-34a-5p promotes trophoblast cell migration and invasion via targetting Smad4. *Bioscience Reports*, *39*(2), BSR20181631. https://doi.org/10.1042/BSR20181631

Yan, Y.-T., Liu, J.-J., Luo, Y., E, C., Haltiwanger, R. S., Abate-Shen, C., & Shen, M. M. (2002). Dual roles of Cripto as a ligand and coreceptor in the nodal signaling pathway. *Molecular and Cellular Biology*, *22*(13), 4439–4449. https://doi.org/10.1128/MCB.22.13.4439-4449.2002

Yeo, C., & Whitman, M. (2001). Nodal signals to Smads through Cripto-dependent and Cripto-independent mechanisms. *Molecular Cell*, *7*(5), 949–957. https://doi.org/10.1016/s1097-2765(01)00249-0

Zeng, Y., Qiu, Y., Jiang, W., Shen, J., Yao, X., He, X., Li, L., Fu, B., & Liu, X. (2022). Biological Features of Extracellular Vesicles and Challenges. *Frontiers in Cell and Developmental Biology*, *10*, 816698. https://doi.org/10.3389/fcell.2022.816698

Zhang, J., Tao, Y., Cai, R., & Wang, Y. (2022). miR-196a-5p-Rich Extracellular Vesicles from Trophoblasts Induce M1 Polarization of Macrophages in Recurrent Miscarriage. *Journal of Immunology Research*, *2022*, 6811632. https://doi.org/10.1155/2022/6811632

Zhang, S., Cao, J., Kong, Y. M., & Scheuermann, R. H. (2010). GO-Bayes: Gene Ontology-based overrepresentation analysis using a Bayesian approach. *Bioinformatics (Oxford, England)*, *26*(7), 905–911. https://doi.org/10.1093/bioinformatics/btq059

Zhou, X., Sasaki, H., Lowe, L., Hogan, B. L. M., & Kuehn, M. R. (1993). Nodal is a novel TGF-β-like gene expressed in the mouse node during gastrulation. *Nature*, *361*(6412), 543–547. https://doi.org/10.1038/361543a0

Zhu, T., Ge, X., Gong, S., Guo, S., Tao, Q., Guo, J., & Ma, R. (2022). Prognostic value of lactate transporter SLC16A1 and SLC16A3 as oncoimmunological biomarkers associating tumor metabolism and immune evasion in glioma. *Cancer Innovation*, *1*(3), 229–239. https://doi.org/10.1002/cai2.32

Zou, J., Chen, Z., Wei, X., Chen, Z., Fu, Y., Yang, X., Chen, D., Wang, R., Jenner, P., Lu, J.-H., Li, M., Zhang, Z., Tang, B., Jin, K., & Wang, Q. (2017). Cystatin C as a potential therapeutic mediator against Parkinson's disease via VEGF-induced angiogenesis and enhanced neuronal autophagy in neurovascular units. *Cell Death & Disease*, *8*(6), e2854. https://doi.org/10.1038/cddis.2017.240